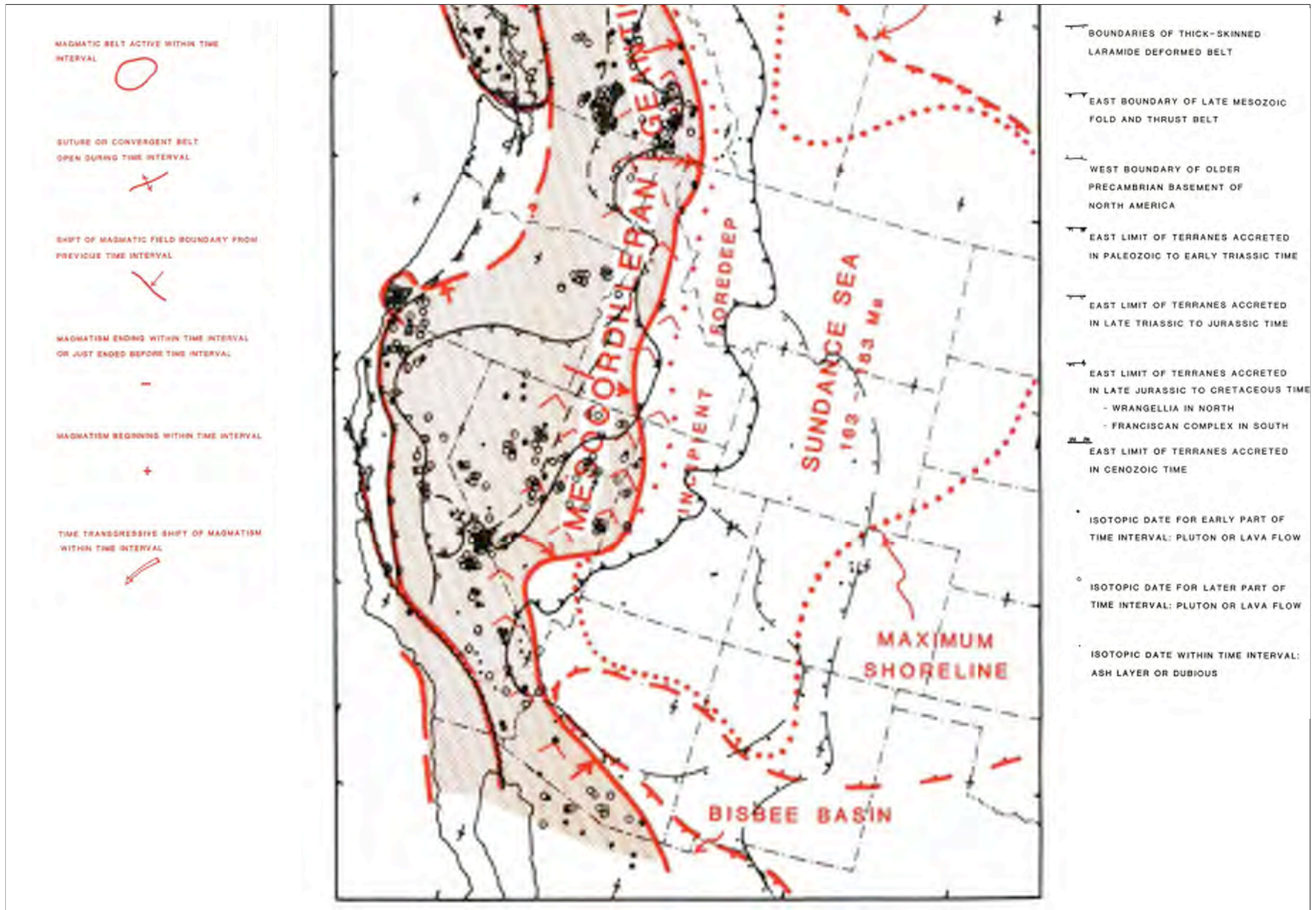

190 Ma to 140 Ma Armstrong and Ward, Geol. Soc. Can SP, 1993

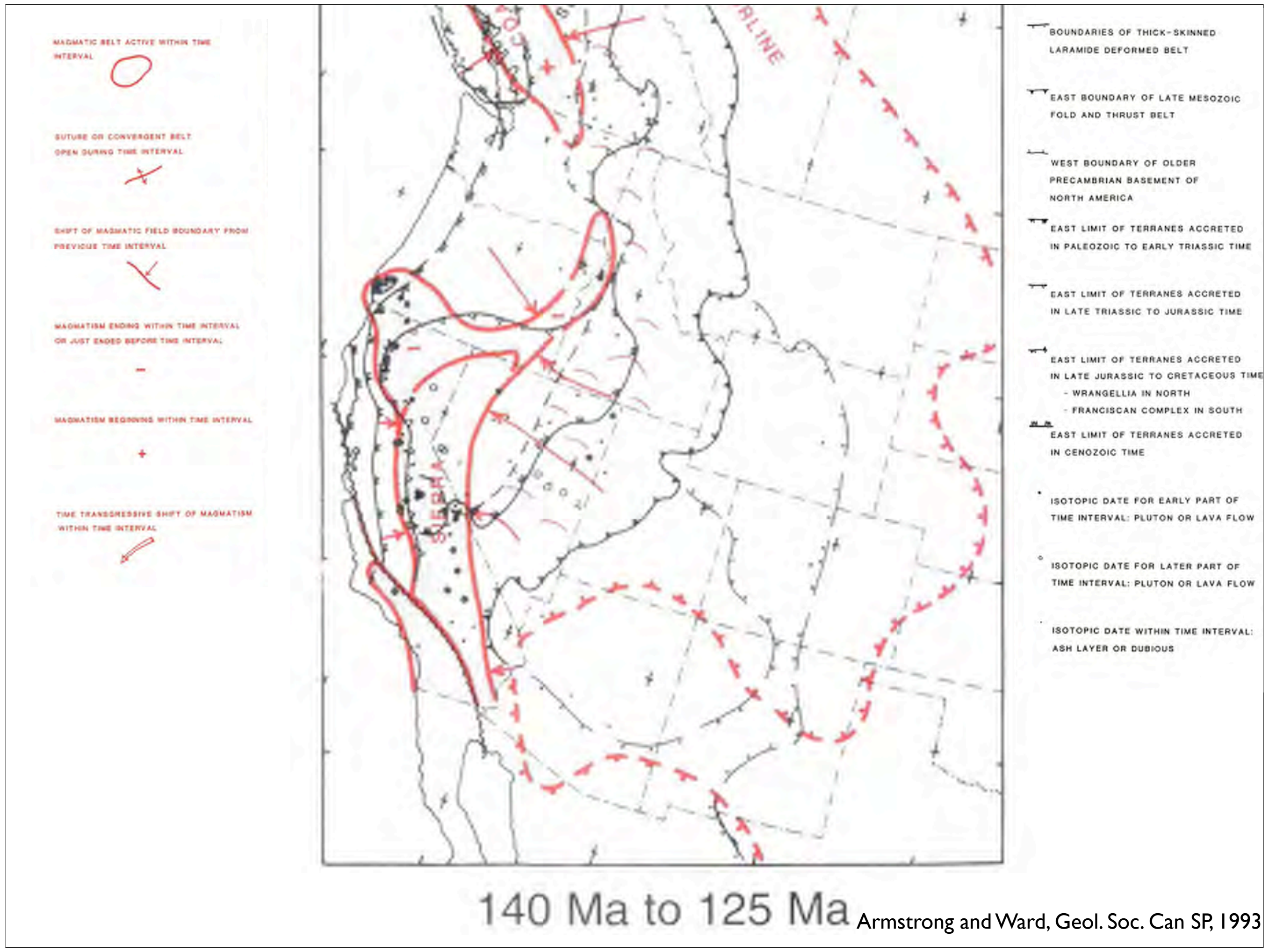

Armstrong and Ward, Geol. Soc. Can SP, 1993

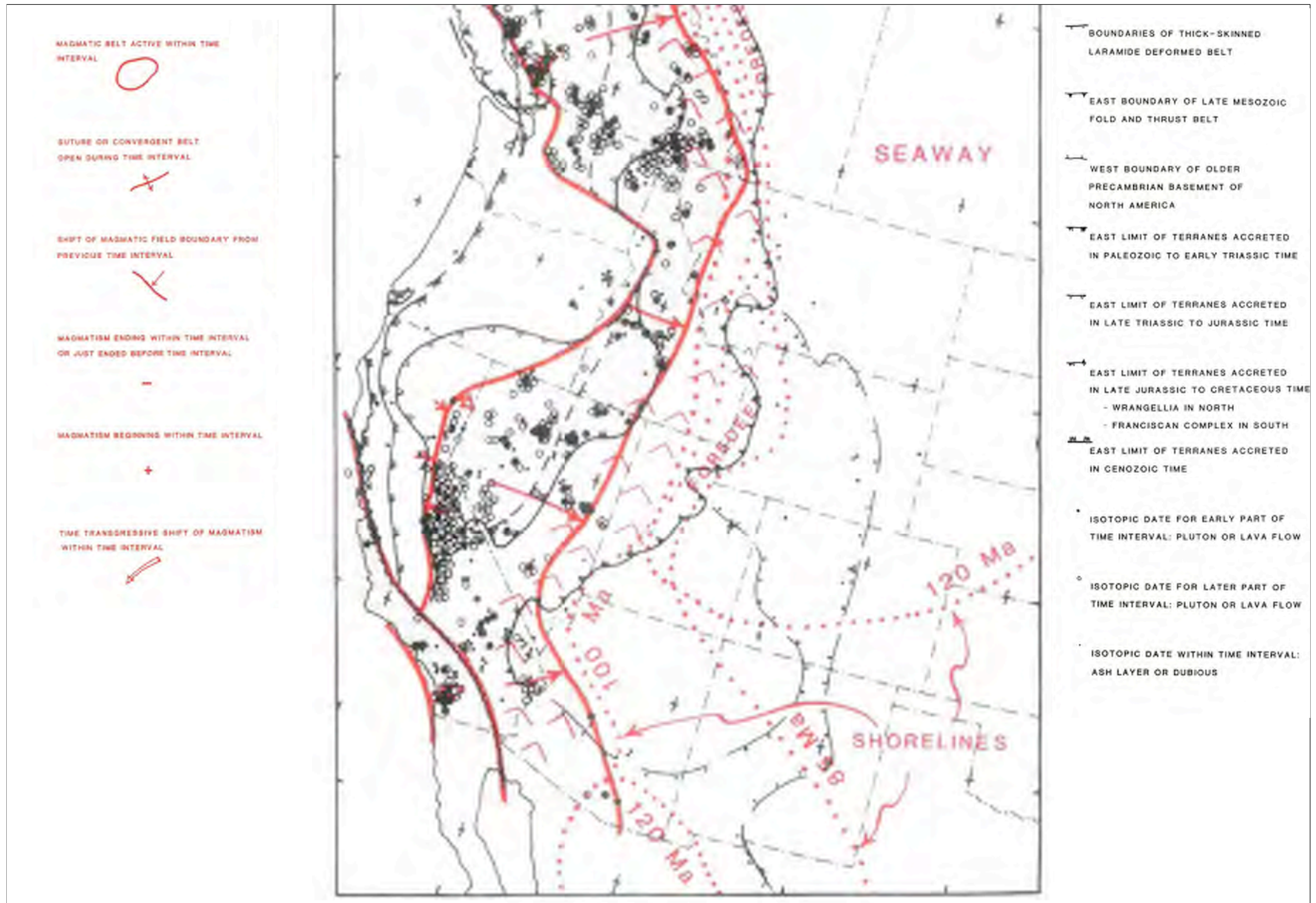

125 Ma to 85 Ma

Armstrong and Ward, Geol. Soc. Can SP, 1993

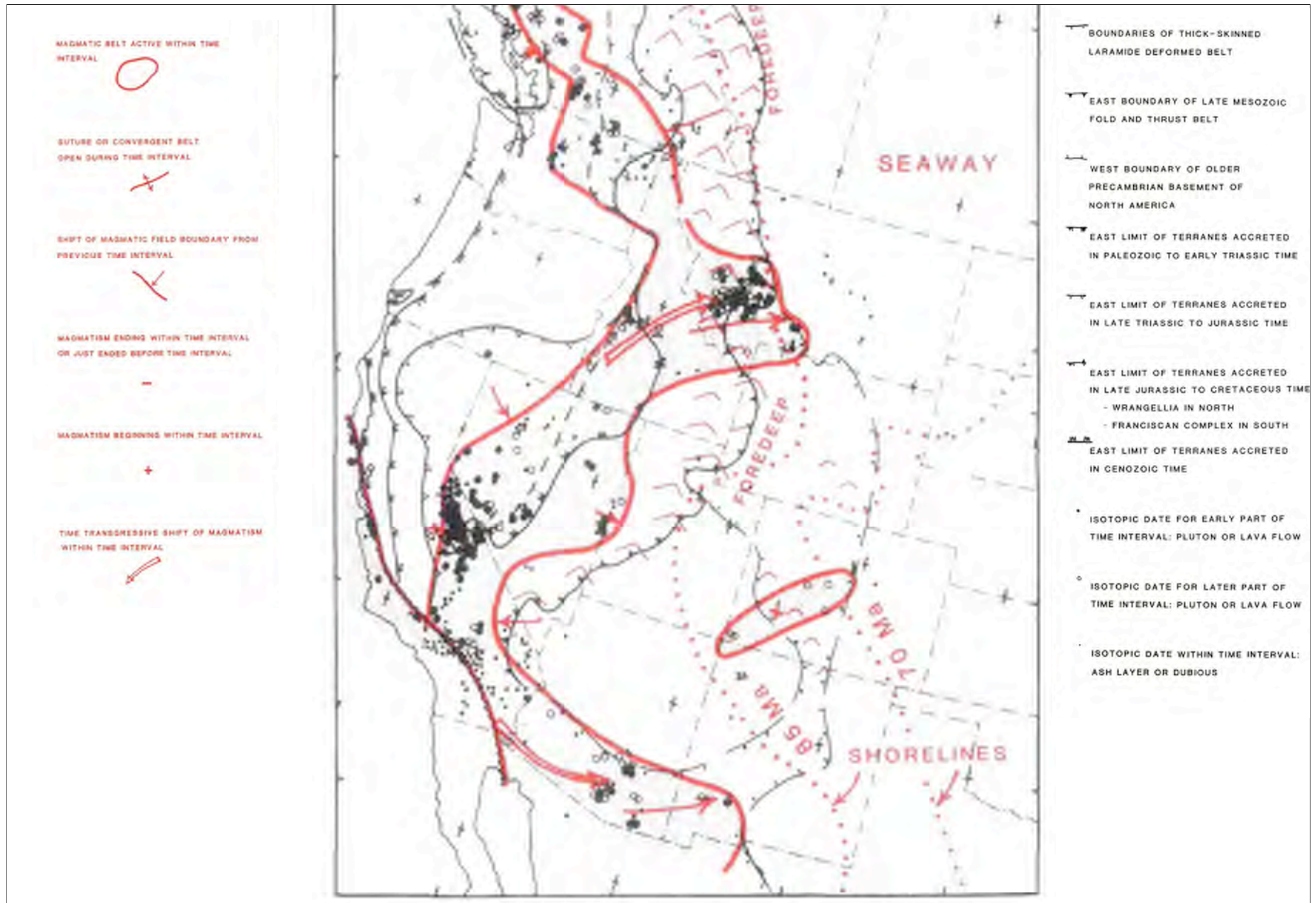

85 Ma to 70 Ma

Armstrong and Ward, Geol. Soc. Can SP, 1993

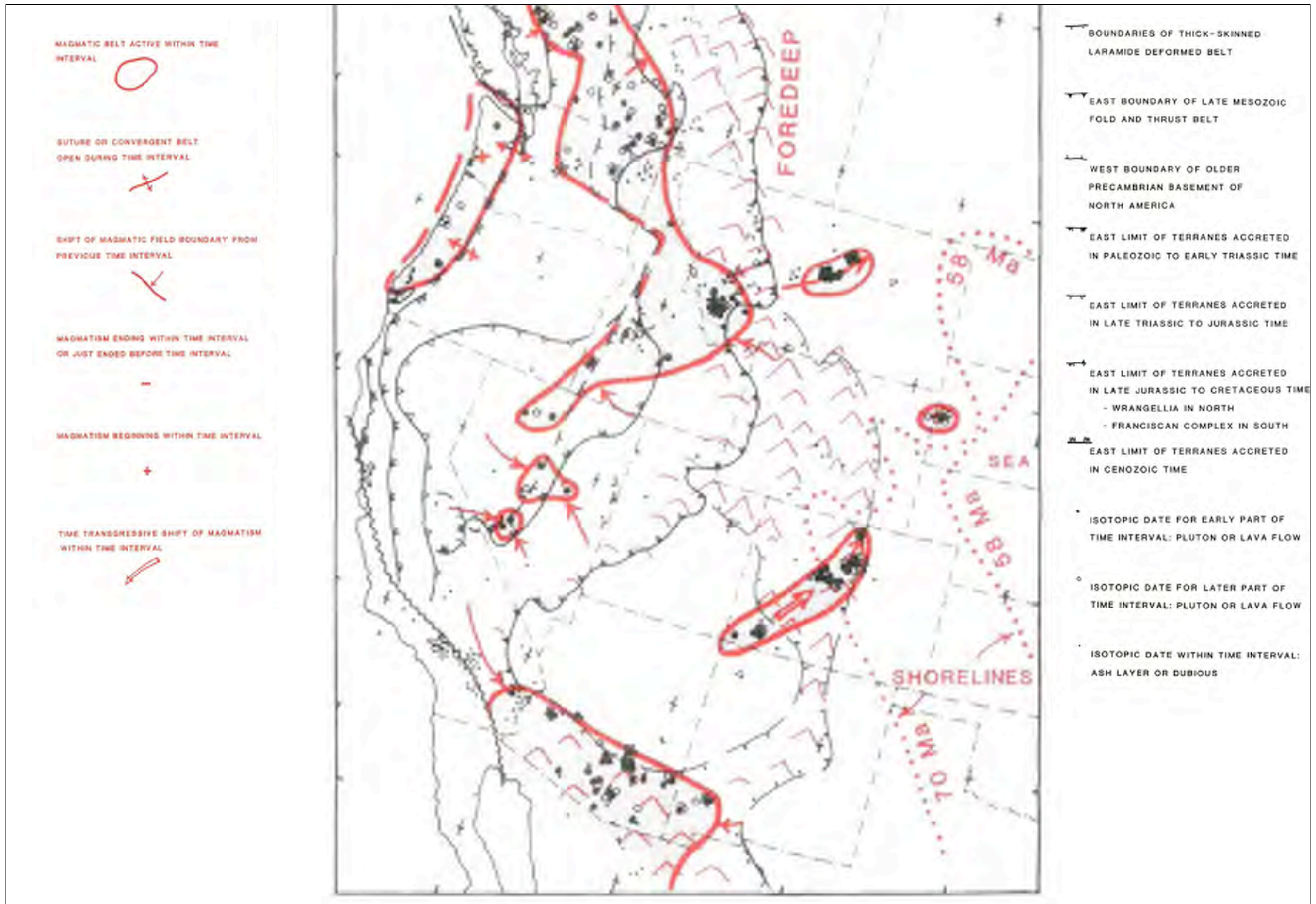

70 Ma to 55 Ma

Armstrong and Ward, Geol. Soc. Can SP, 1993

Slab depth under volcanic arc fronts

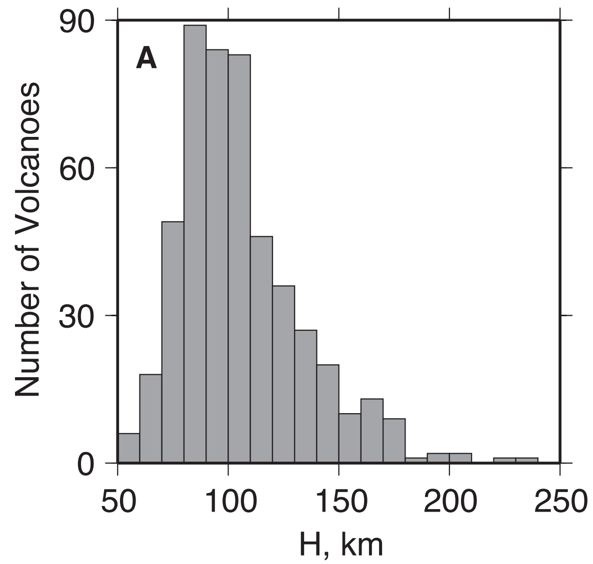

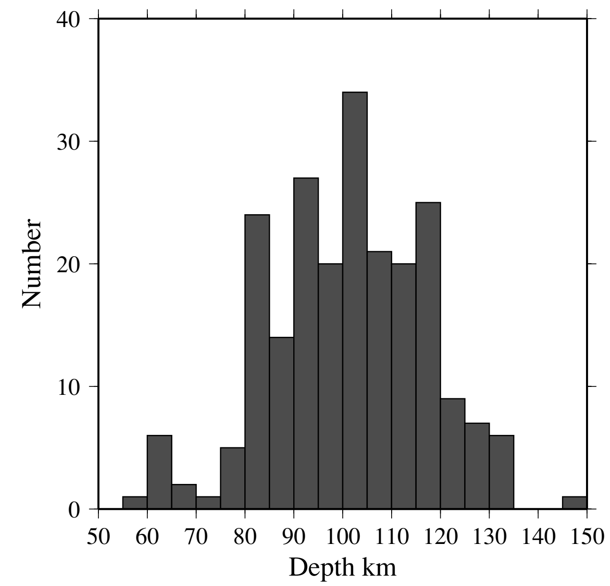

Syracuse & Abers, G^3, 2006

England et al., *GJI*, 2004

A lot of the variation is apparently most closely related to the vertical descent rate (V * sin(dip)).

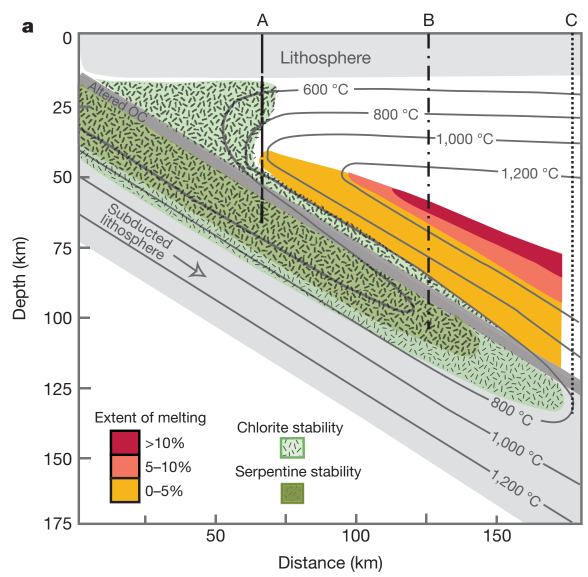

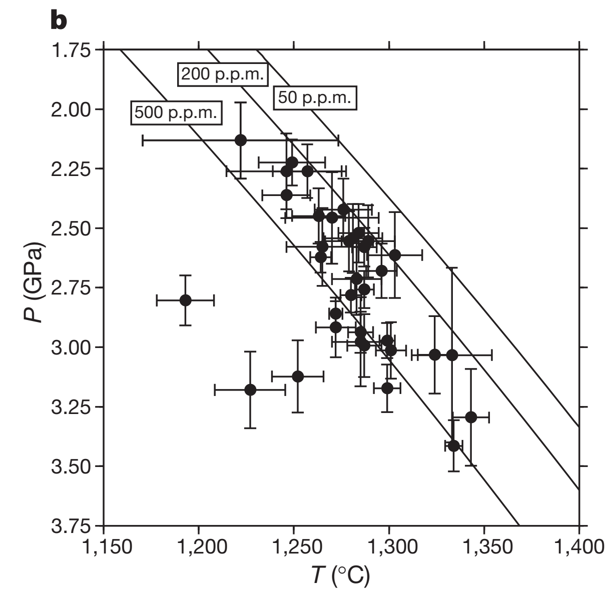

Maximum temperature in wedge

Grove et al., *Nature*, 2009

England and Katz., *Nature*, 2010

Exact mechanism for this relation is debated still, but increasingly seems like the temperature in the mantle wedge is what controls this

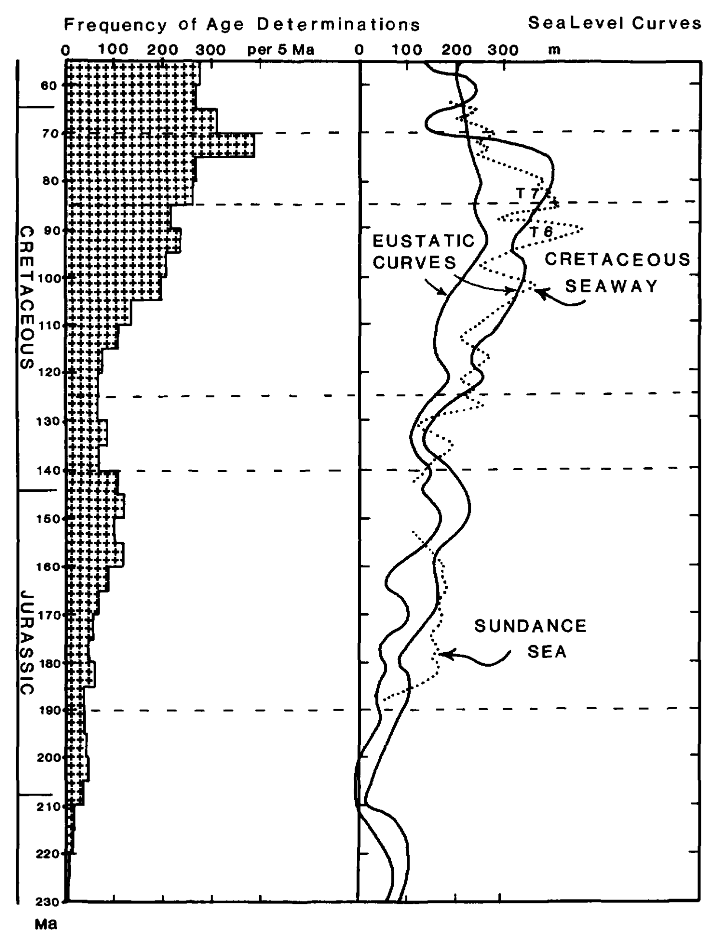

Figure 1. *Comparison of the frequency of isotopic dates between 230 Ma and 55 Ma for magmatic rocks in the North American Cordillera (from RADB and Canadian Cordilleran Isotopic Data File) between the northern border of Mexico and the western border of Yukon Territory, and sea-level curves from several sources. The worldwide eustatic sea-level curves are from Haq* et al. *(1987) and Hallam (1984) (who gives somewhat higher estimates of eustatic sea-level rise), and show the general agreement on broad trends, but the uncertainty of some details. The Cretaceous seaway transgression-regression curve is modified from Kauffman (1985) and the Sundance Sea curve derived from Imlay (1980).*

Armstrong and Ward, Geol. Soc. Can SP, 1993

At the broadest level (all of North America), it would seem that magmatism is pretty constant...

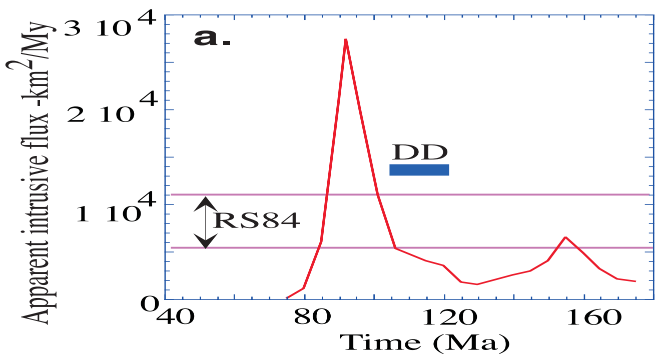

Southern Sierran plutons

Ducea, GSA Today, 2001

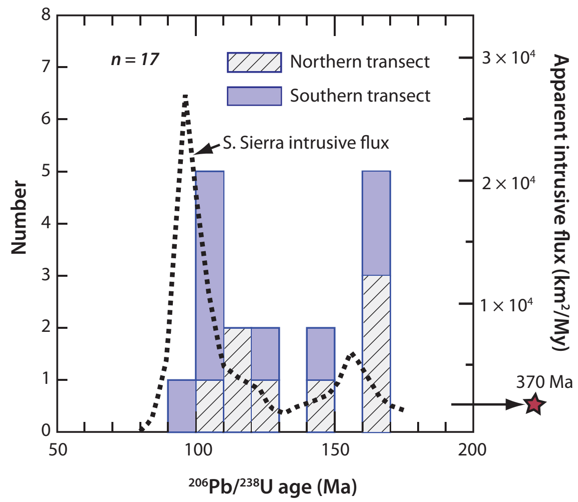

Northern Sierra plutons

Robinson et al, *Geosphere*, 2012

Observationally, arc (expressed as plutons) at any one latitude seems to vary in intensity (though it is unclear if this captures the full E–W extent of arc)

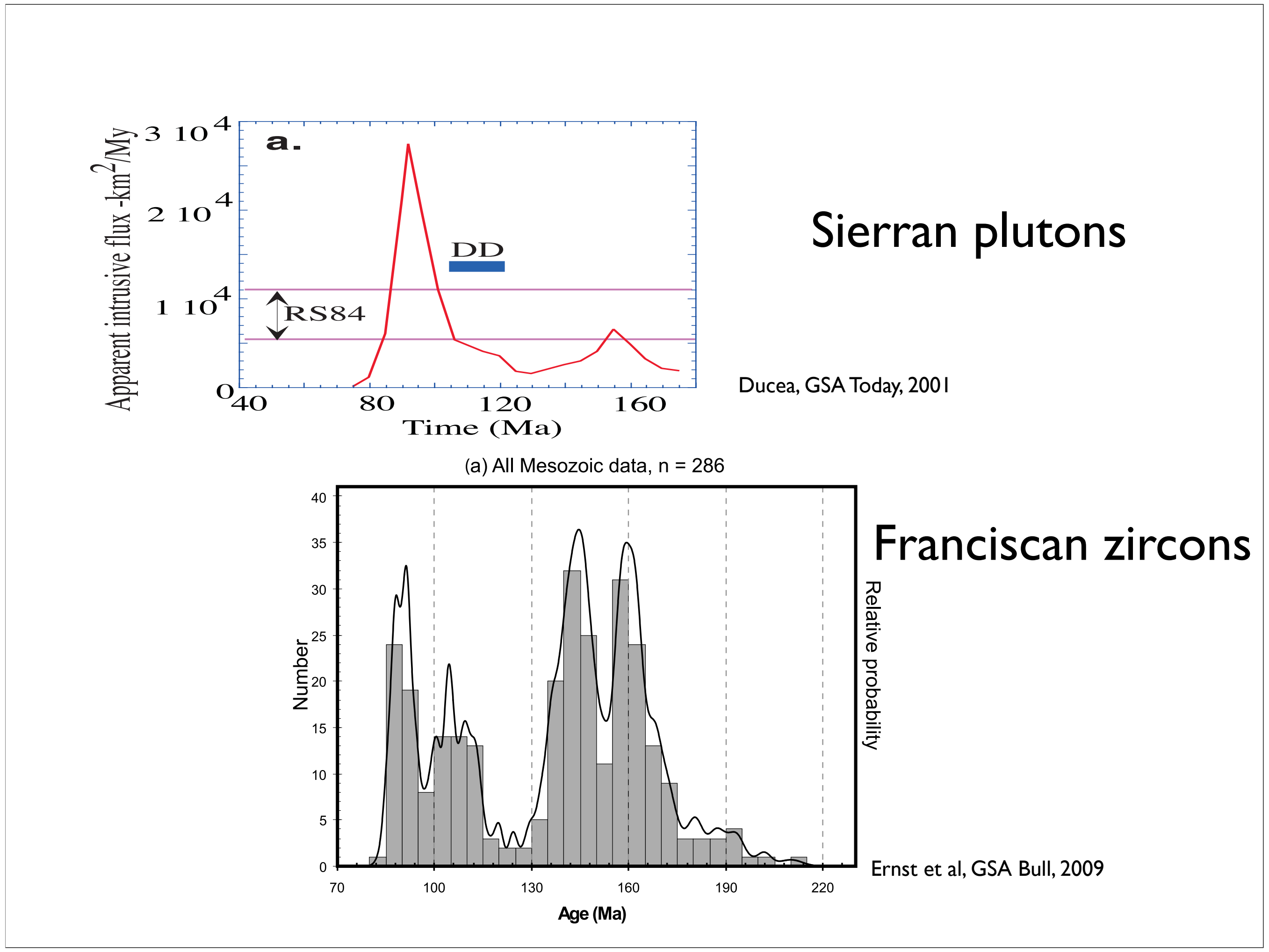

Ernst zircons from metagraywackes dating from ~102 to ~85 Ma.

Ducea: Plot of total California arc apparent intrusive flux (area of presently exposed plutonic rocks produced per units of time; in km^2/m.y.) vs. time of magmatism, using an updated version of CONTACT88 (Barton et al., 1988). About 600 plutons representing almost 65% of arc-exposed area have been included in database. Line labeled DD indicates period of ductile deformation in exposed mid-crust of arc and in granulite xenoliths. RS84 corresponds to magmatic addition rates in range of 20–40 km^3/km • m.y., typical of island arcs (Reymer and Schubert, 1984). Magmatic addition rate is defined as total volume of magma produced in an arc per unit of time scaled over length of arc, assuming an average granitoid thickness of 30 km for California arc.

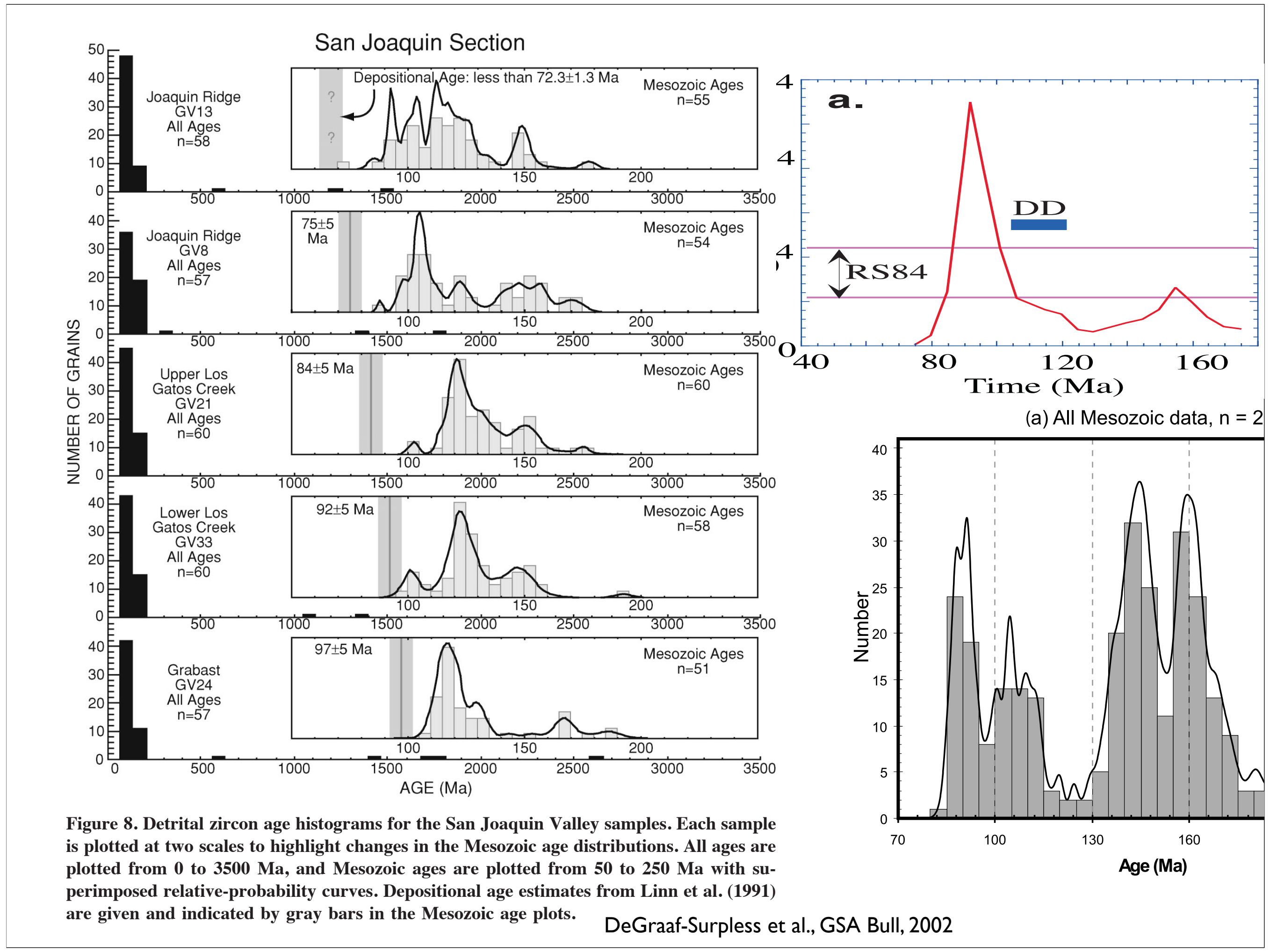

Figure 8. Detrital zircon age histograms for the San Joaquin Valley samples. Each sample is plotted at two scales to highlight changes in the Mesozoic age distributions. All ages are plotted from 0 to 3500 Ma, and Mesozoic ages are plotted from 50 to 250 Ma with superimposed relative-probability curves. Depositional age estimates from Linn et al. (1991) are given and indicated by gray bars in the Mesozoic age plots.

DeGraaf-Surpless et al., GSA Bull, 2002

Detrital zircons from Coalinga area (southern Coast Ranges) show a significant source in 120 Ma window that seems absent in batholith—could be plutons now buried under Great Valley that Saleeby has spoken about at a few meetings. So a bit of a challenge in terms of understanding arc evolution. Other site in northern Coast Ranges doesn't see the 120 Ma spike…

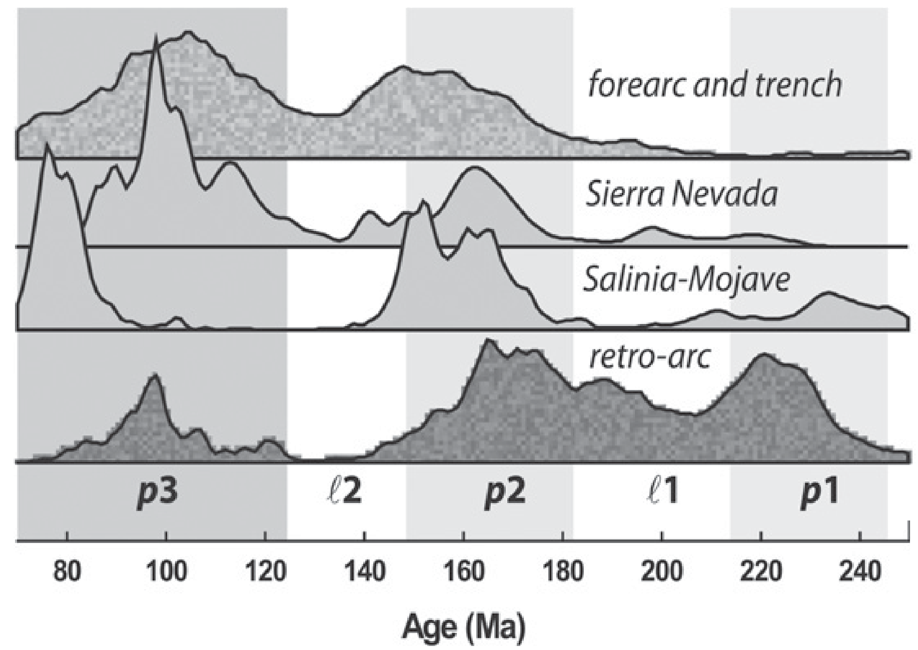

Barth et al., *Geology*, 2013

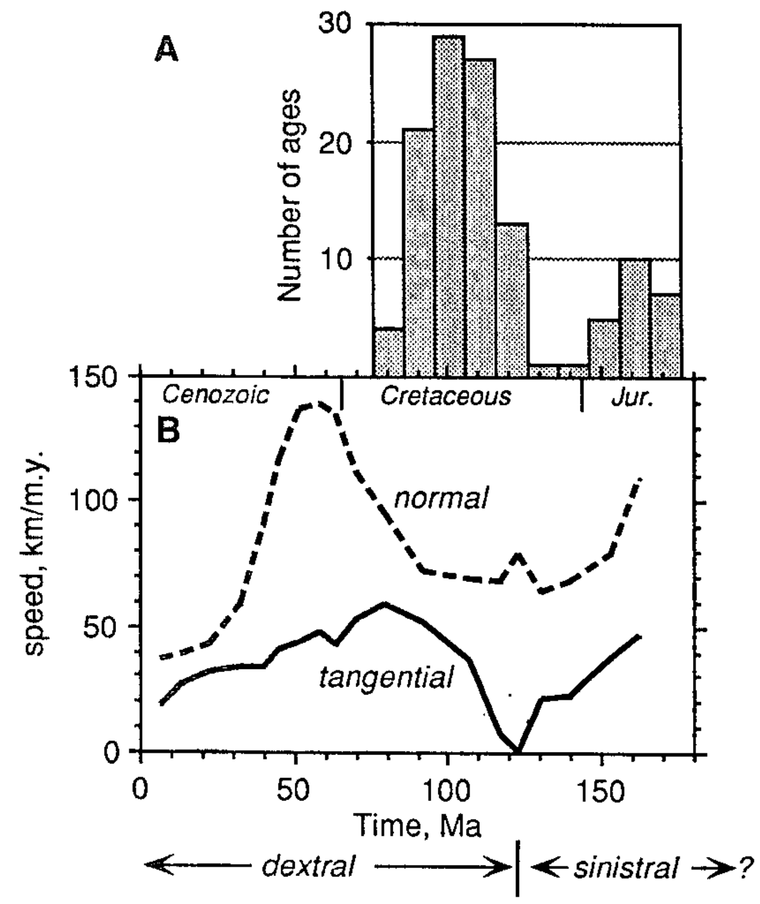

Figure 1. A: Histogram of U-Pb zircon ages from plutonic rocks from California. Data from Stern et al. (1981), Chen and Moore (1982), and Silver and Chappell (1988). Although these data are imperfect representation of relative volumes of plutonic rocks, they indicate significant Late Jurassic and Cretaceous fluxes, separated by earliest Cretaceous lull. B: Normal and tangential components of convergence between Farallon and North American plates, calculated from data of Engebretson et al. (1985) (see text). Curves were smoothed by three-point moving average. Note that predicted time of change from sinistral to dextral convergence correlates with lull in plutonism. Exact time of change depends on assumed orientation of trench; sense of movement predicted by reconstructions is consistent with geologic data (see text). Period boundaries from Harland et al. (1982).

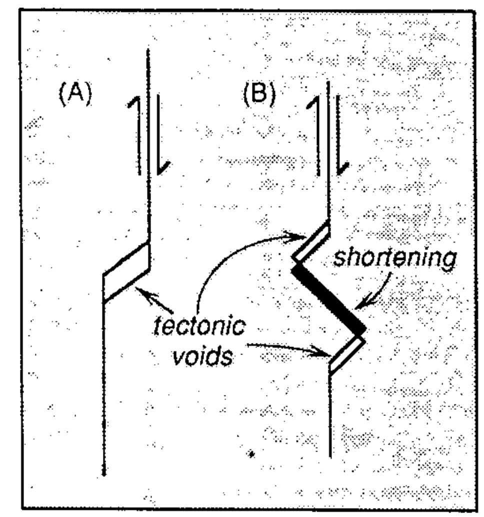

Glazner, Geology, 1991

but within arcs, there seems to be episodic instances of major plutonic activity...maybe due to changes in ability to emplace plutons?

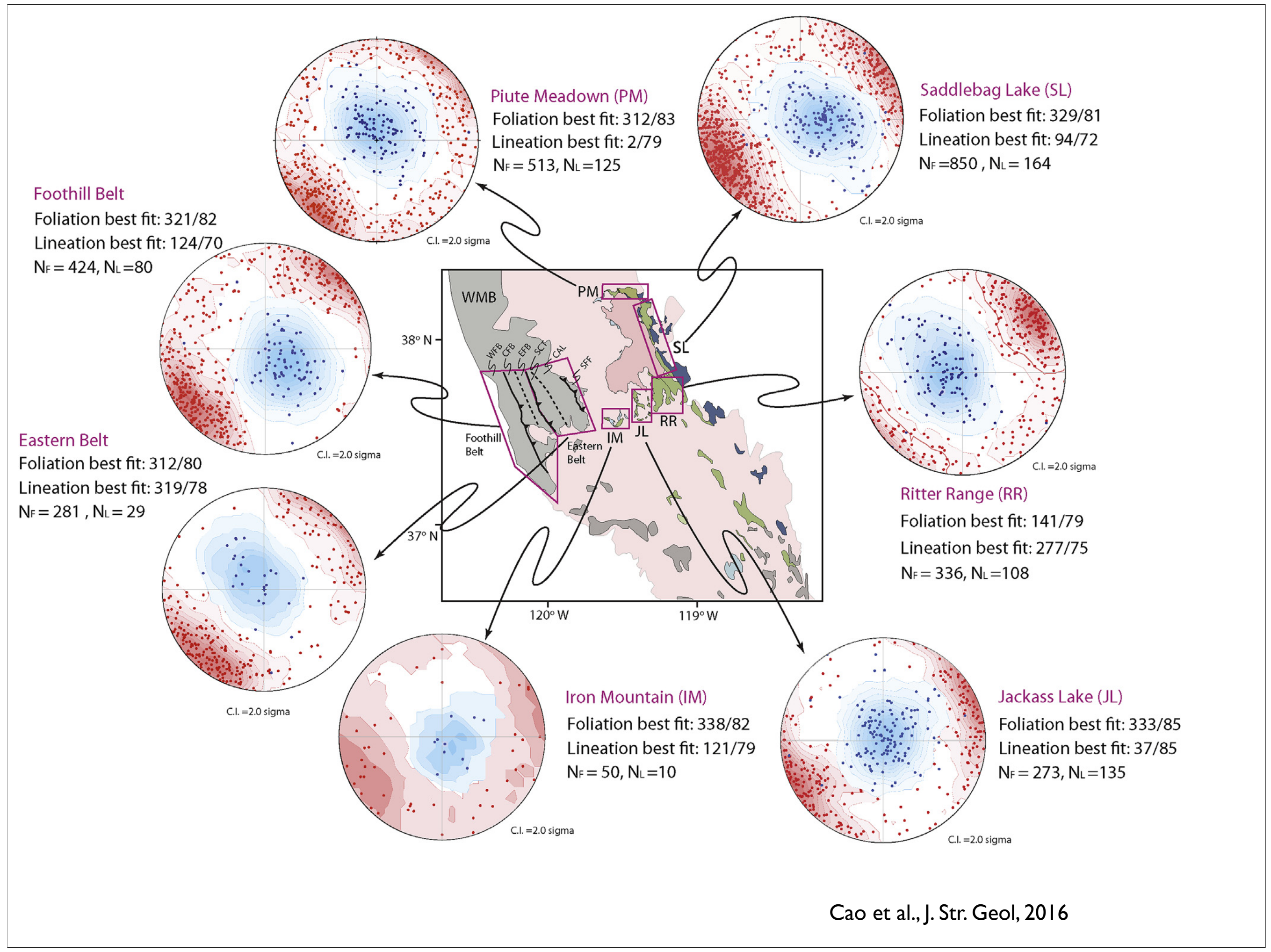

Structural work in the Sierra points to vertical elongation and arc-normal shortening.

Fig. 3. Lower hemisphere, equal area projections of metamorphic foliations and lineations from Western Metamorphic Belt and host rock pendants in central Sierra Nevada. Kamb contours with 2.0 sigma contour interval (C.I.) are added. Dots in the red shade are poles to the metamorphic foliation and dots in the blue shade are metamorphic lineation. N_F Number of foliation, N_L Number of lineation. Cylindrical best fits are calculated using Stereonet 9.0 and 95% confidence ellipses (Allmendinger et al., 2012; Cardozo and Allmendinger, 2013).

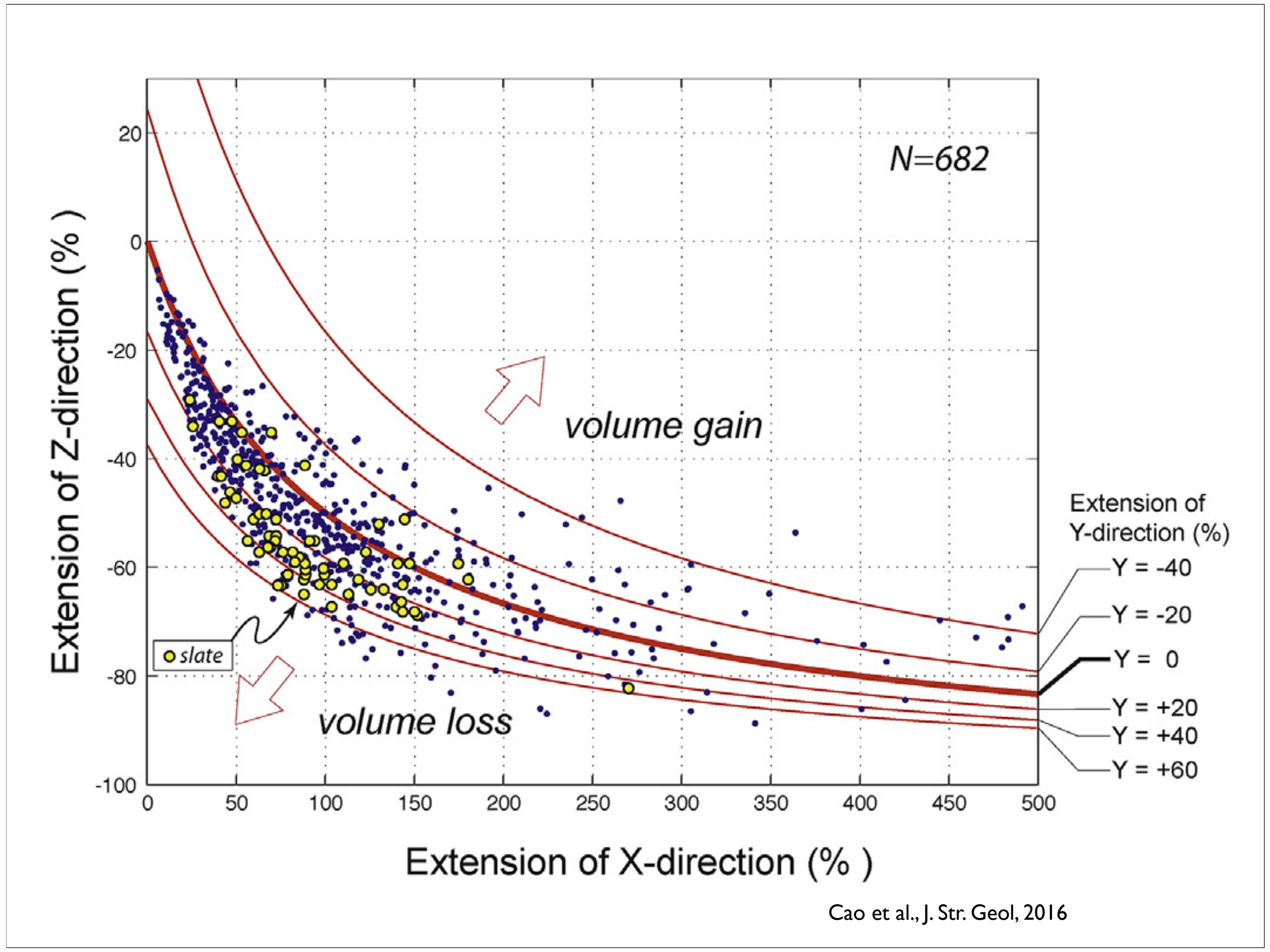

Note Z is maximum shortening (so arc-normal here) and X is maximum elongation (vertical). Note volume loss/gain trades off with extension/shortening along Y axis.

Fig. 5. Finite strain measurements plotted in the space of X- and Z-extension percent (negative value ¼ shortening; X, Y, Z are the longest, intermediate and shortest axes of a finite strain ellipsoid). Each dot represents an individual strain measurement. The central coarse red curves represent the relation between X- and Z-extension if the deformation is plane strain. The thin red curves represent the relation between X- and Z-extension if there is volume loss or Y-extension during deformation. Measurements from slates are shown as yellow dots, whose finite strain ellipsoids are likely to be affected by primary compaction during sedimentation and lithification. The plot suggests that the host rocks in the central Sierra Nevada are strained at about 50% in average with <15e20% Y-direction length change and/or potential volume changes.

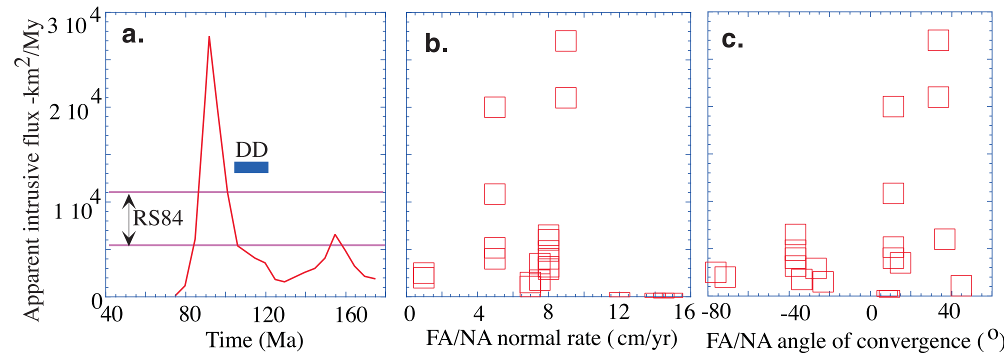

Figure 6. A: Plot of total California arc apparent intrusive flux (area of presently exposed plutonic rocks produced per units of time; in km²/m.y.) vs. time of magmatism, using an updated version of CONTACT88 (Barton et al., 1988). About 600 plutons representing almost 65% of arc-exposed area have been included in database. Line labeled DD indicates period of ductile deformation in exposed mid-crust of arc and in granulite xenoliths. RS84 corresponds to magmatic addition rates in range of 20–40 km³/km • m.y., typical of island arcs (Reymer and Schubert, 1984). Magmatic addition rate is defined as total volume of magma produced in an arc per unit of time scaled over length of arc, assuming an average granitoid thickness of 30 km for California arc. **B:** Plot of apparent intrusive flux vs. normal convergence rate between Farallon and North American plates in California (Page and Engebretson, 1985) for 5 m.y. intervals between 170 and 60 Ma. **C:** Plot of apparent intrusive flux vs. angle of convergence in degrees. Zero corresponds to normal convergence, positive angles reflect right-lateral motion, and negative angles represent left-lateral motion.

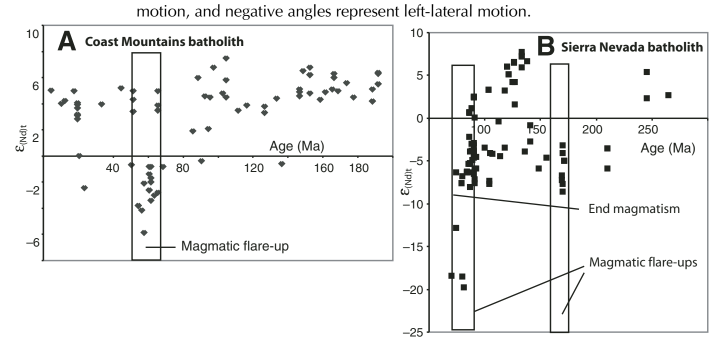

Figure 2. Initial ε_{Nd} whole rock values, as a function of crystallization age for plutons in the (A) Coast Mountains batholith (British Columbia) and (B) Sierra Nevada batholith. Ducea & Barton, *Geology*, 2007

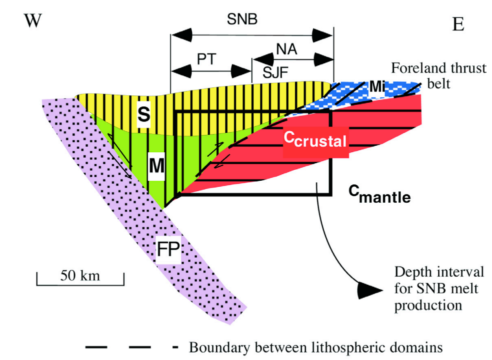

Ducea, *GSA Today*, 2001

Estimates of intrusive flux inferred to be episodic…maybe related to obliquity? (Which was kind of what Glazner was going for). Notes ENd seems related to flux: high flux when End low…so cartoon at lower right.

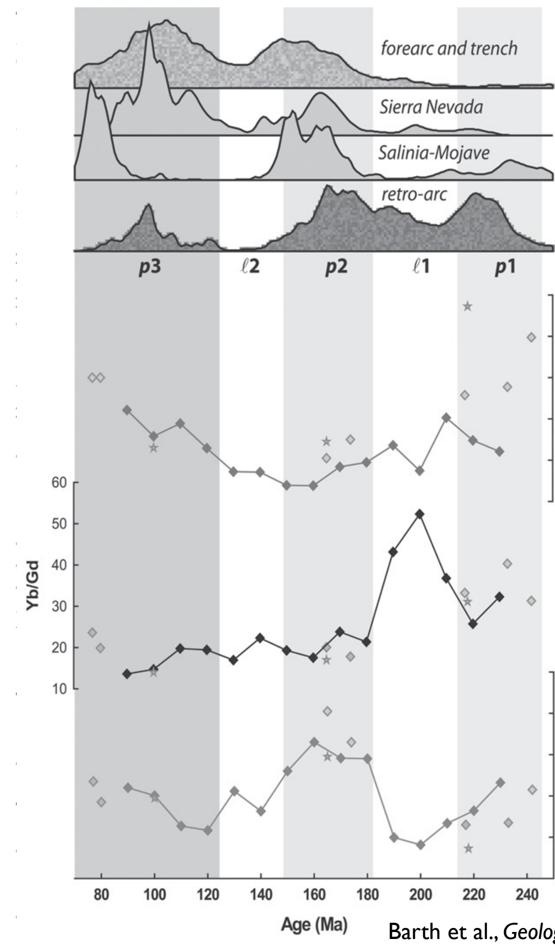

Barth et al., *Geology*, 2013

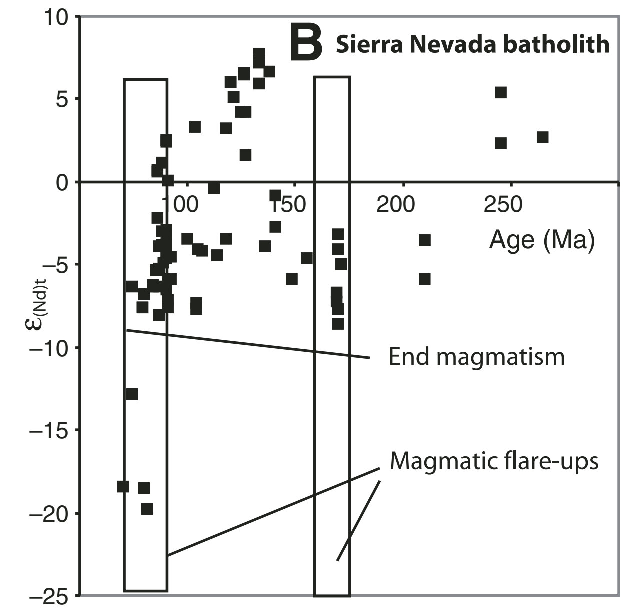

Ducea & Barton, *Geology*, 2007

Ratios from detrital zircons (solid lines) and magmatic zircons (points) Interpret the decreasing Yb/Gd as increasing crustal influence (basically, garnet is increasingly involved as a residue, requiring thicker crust); Th/U high in higher volume episodes requires crustal input. Lull 1 maybe related to extension (little slab derived fluid + little crustal involvement [GSA talk 2016 claimed there was nothing significantly different in lulls–Hernandez et al. poster Tuesday afternoon]

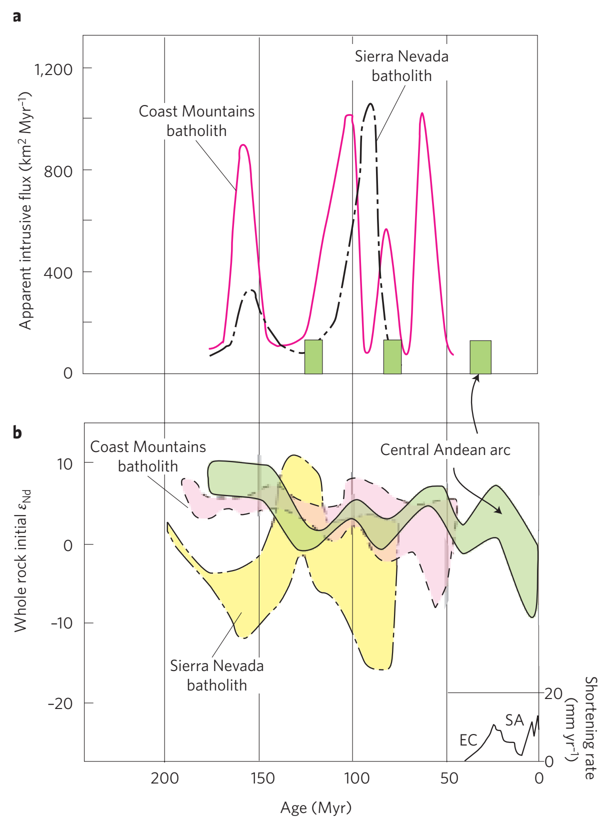

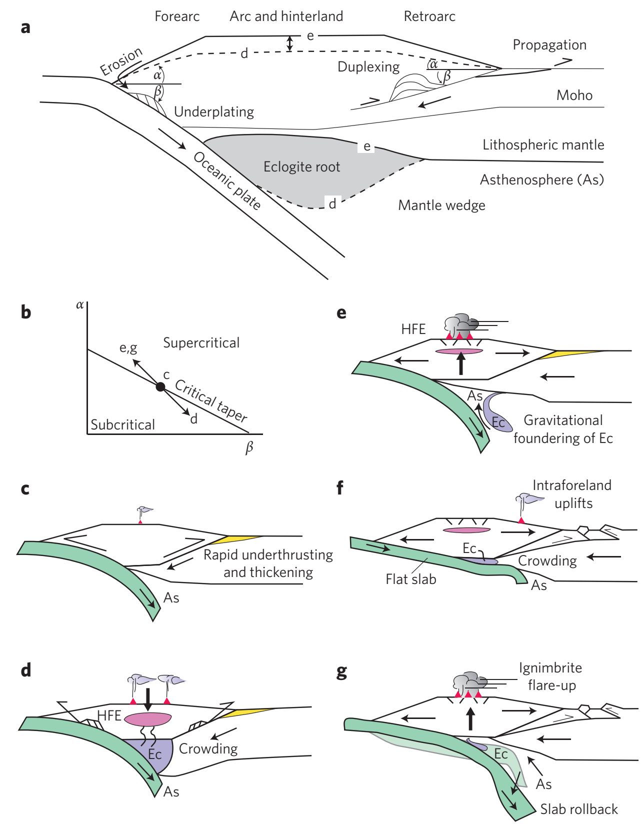

DeCelles et al., *Nature Geosci.*, 2009

Figure 3 l evolution of Cordilleran orogenic systems. a, Schematic cross- section (not to scale) of a Cordilleran orogenic system with a sediment- starved trench, illustrating the effects of eclogite root development and removal on isostatic and orogenic wedge taper ($\alpha + \beta$). For clarity, the magmatic arc is omitted. All lettered labels refer to other parts of this figure. Dashed lines labelled d represent the topographic profile and base of the lithosphere configuration at the peak of eclogite (gray shading) growth. Solid lines labelled e show post-drip/delamination configurations, in which the base of the lithosphere is adjusted upward and the surface has rebounded to high elevation. Kinematic processes responding to changes in orogenic wedge taper (duplexing and underplating) are also illustrated. b, Critical taper diagram in terms of surface slope (α) and the angle of the basal detachment (β) depicting the evolution of taper in forearc and retroarc orogenic wedges at different stages of the cycle. The dot labelled c represents a given orogenic wedge at the critical taper (the straight line with negative slope), and arrows indicate taper changes corresponding to configurations labelled in part a, and illustrated in cross sections c–g of this figure. c, Retroarc underthrusting. d, Development of an arc HFE and growth of the eclogite root (Ec) beneath the arc causing a regional isostatic depression of surface elevation, and internal underplating and duplexing in the forearc and retroarc wedges. e, Eclogite root foundering, regional uplift and outward propagation of the flanking orogenic wedges, upper- crustal extension and ignimbrite flare-up. Subduction of a buoyant oceanic slab immediately after stage e would potentially produce the situation illustrated in f, where flat-slab subduction creates crowding beneath the arc and drives strain into the foreland region. As the slab returns to a normal subduction angle g, upwelling asthenosphere (As) may promote a regional ignimbrite flare-up.

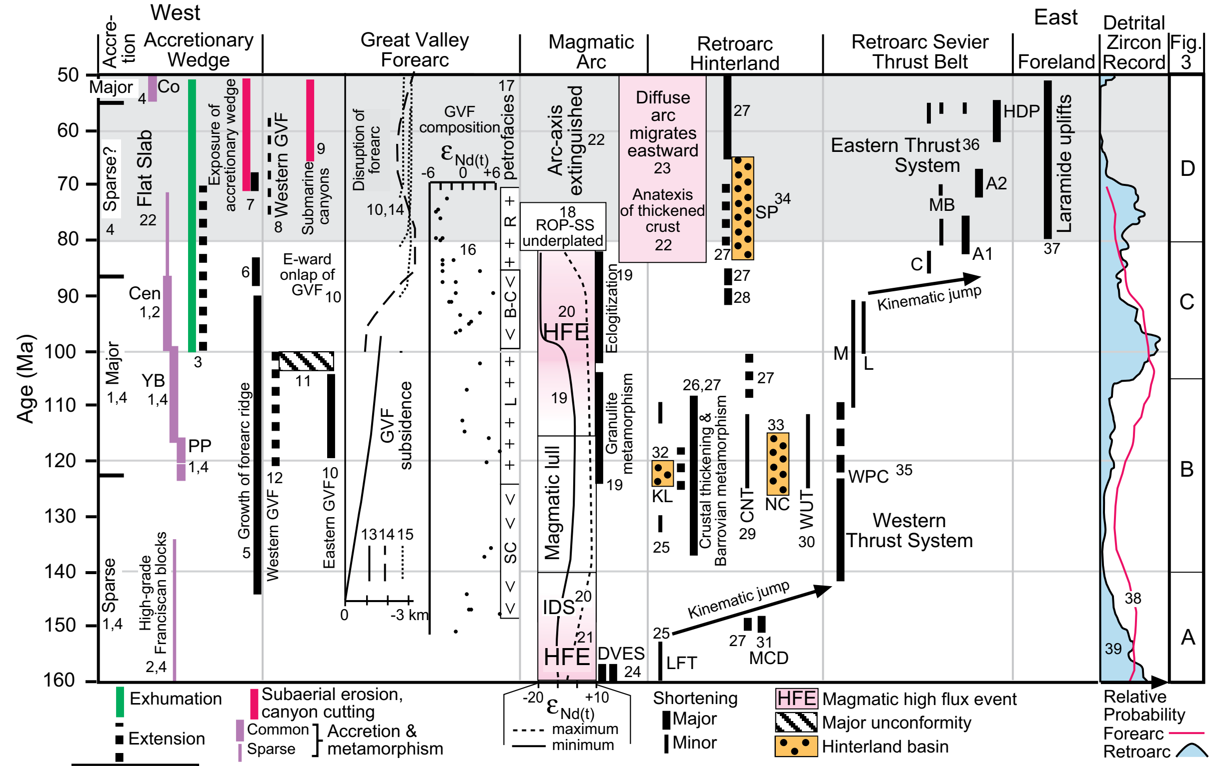

Abbreviations:

GVF petrofacies: + = Quartzo-Feldspathic, ∨ = Volcanic-Rich

PP, Pickett Peak terrane
YB, Yolla Bolly terrane
Cen, Central Belt
Co, Coastal Belt
GVF, Great Valley forearc basin
IDS, Independence dike swarm
ROP-SS, Rand-Orocopia-Pelona & Sierra de Salinas schists
DVES, Death Valley-Eastern Sierra thrust belts
LFT, Luning-Fencemaker thrust belt
MCD, Manning Canyon detachment
CNT, Central Nevada thrust belt
WUT, Western Utah thrust belt
NC, Newark Canyon basin
SP, Sheep Pass basin
KL, King Lear basin
WPC, Willard-Paris-Canyon Range thrusts
M, Meade thrust
L, Laketown thrust
C, Crawford thrust
MB, Medicine Butte thrust
A1, A2, Early and Late Absaroka thrusts
HDP, Hogsback-Darby-Prospect thrusts
GVF Petrofacies: SC, Stony Creek; L, Ladoga; B-C, Boxer-Cortina; R, Rumsey

DeCelles and Graham, *Geology* 2015

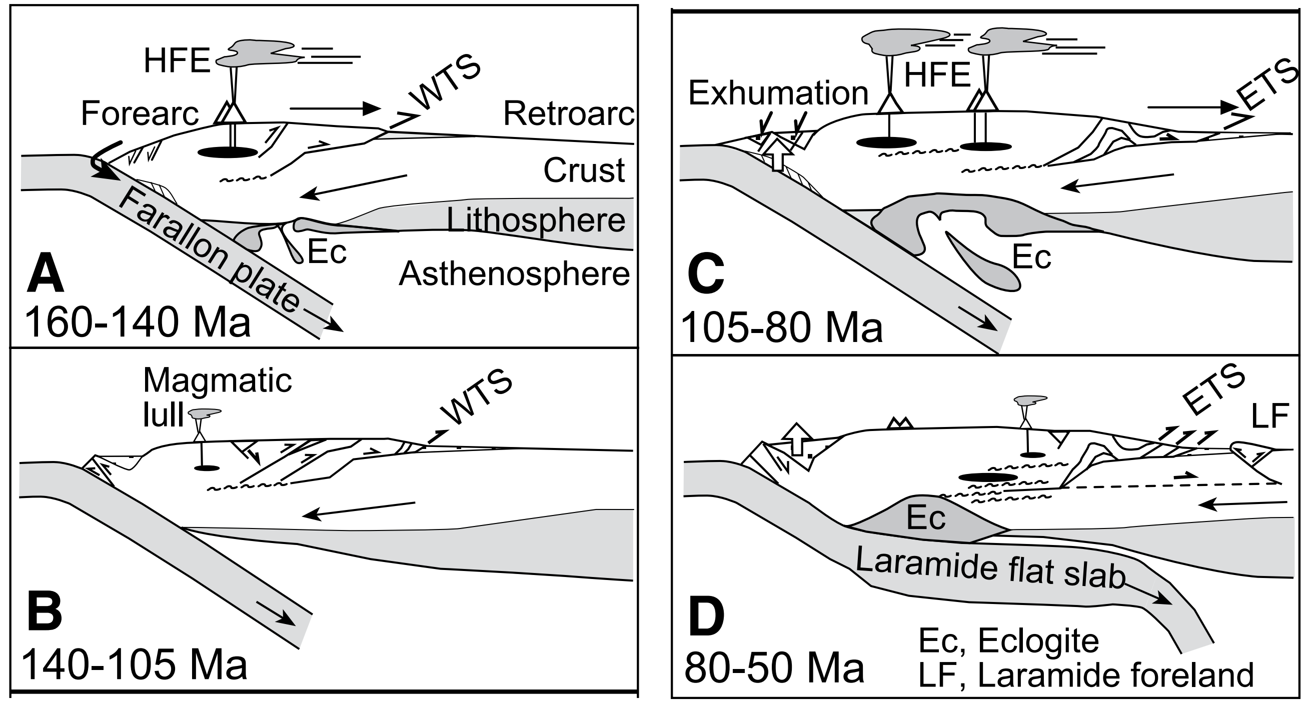

DeCelles and Graham, *Geology* 2015

Proposed cycle

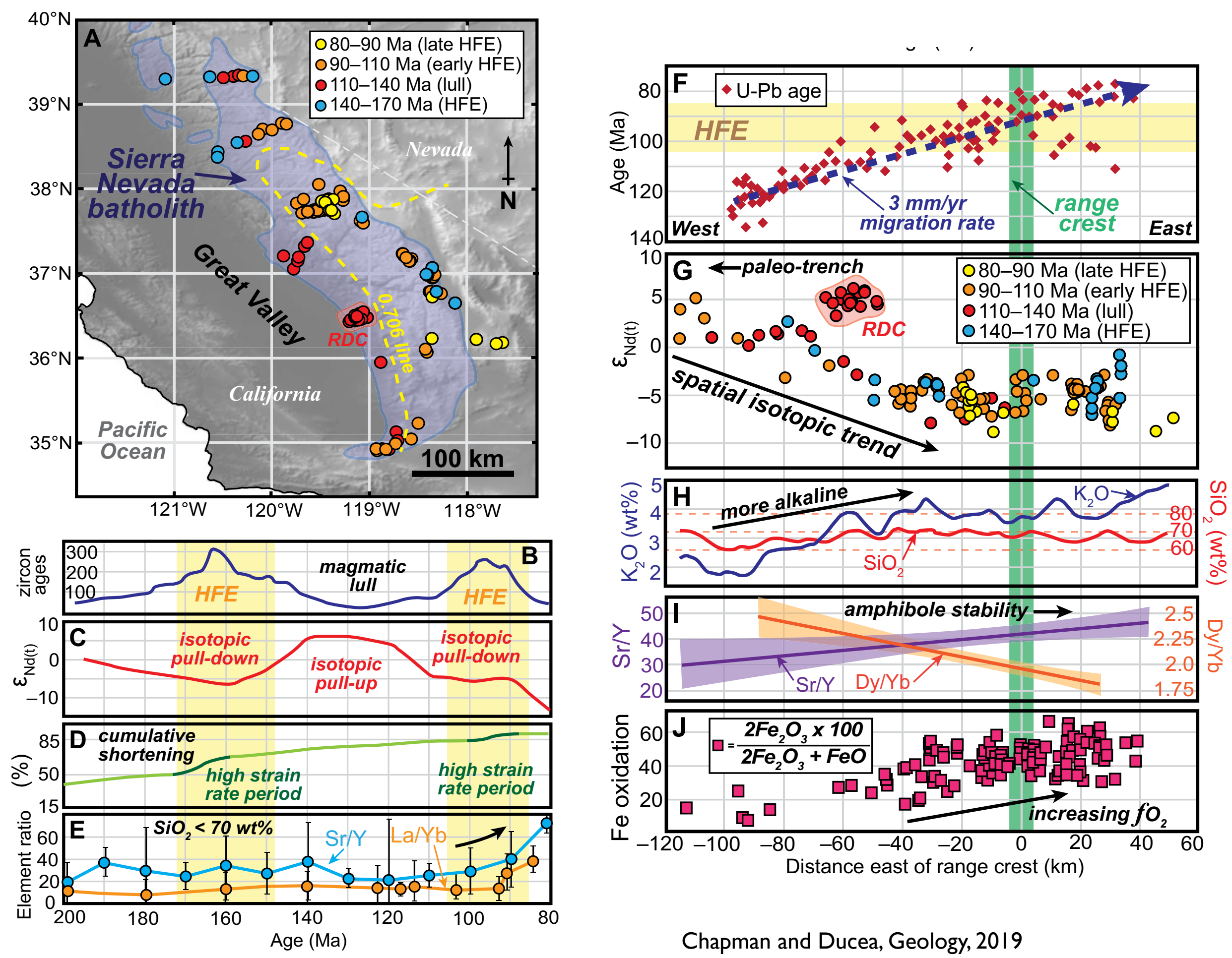

Chapman and Ducea, Geology, 2019

More cycles. Note HFE = High Flux Event. MIgration of the arc tied to last HFE, lower E_{Nd}. Note appearance of Sr/Y

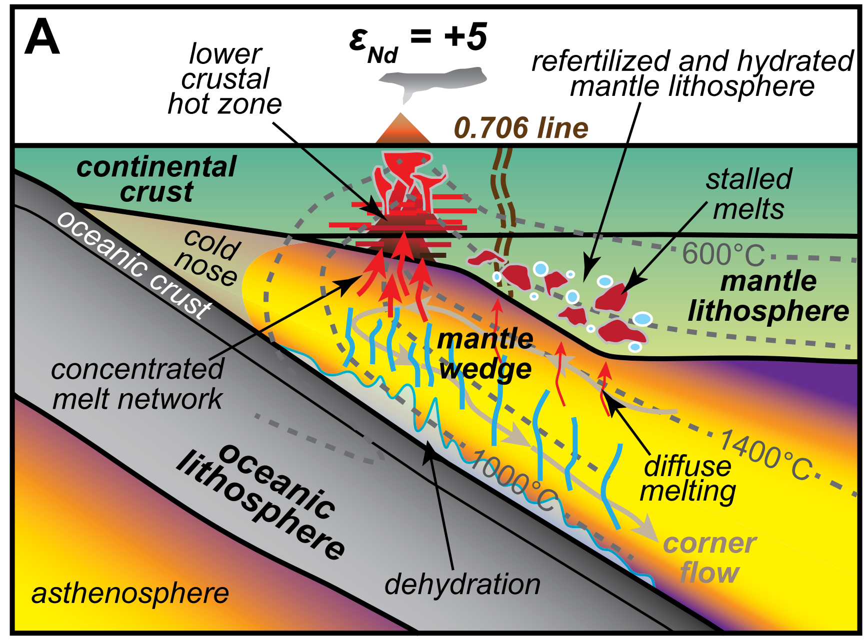

Chapman and Ducea, Geology, 2019

More cycles. Note HFE = High Flux Event. MIgration of the arc tied to last HFE, lower E_{Nd}.

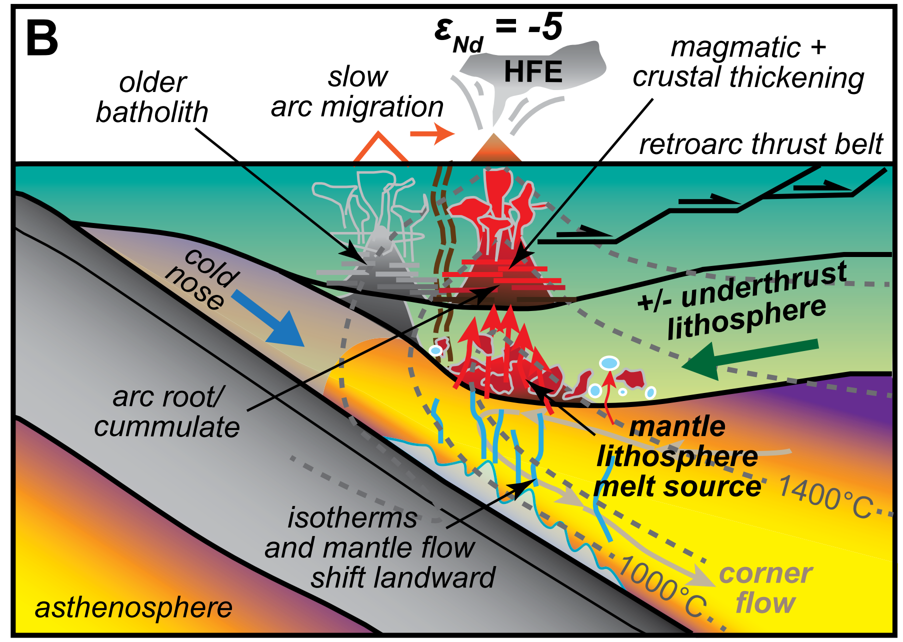

Chapman and Ducea, Geology, 2019

More cycles. Note HFE = High Flux Event. MIgration of the arc tied to last HFE, lower E_{Nd}.

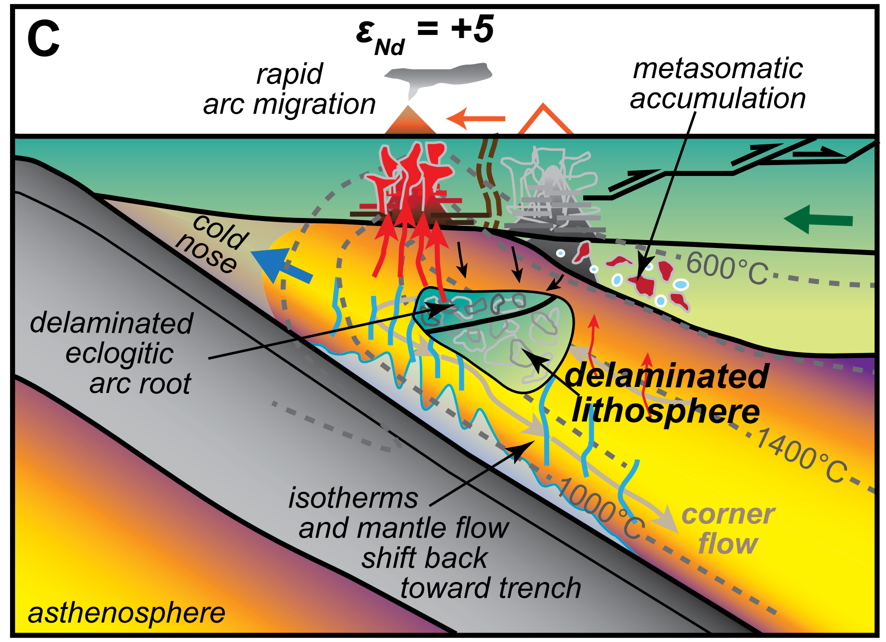

Chapman and Ducea, Geology, 2019

More cycles. Note HFE = High Flux Event. MIgration of the arc tied to last HFE, lower E_{Nd}.

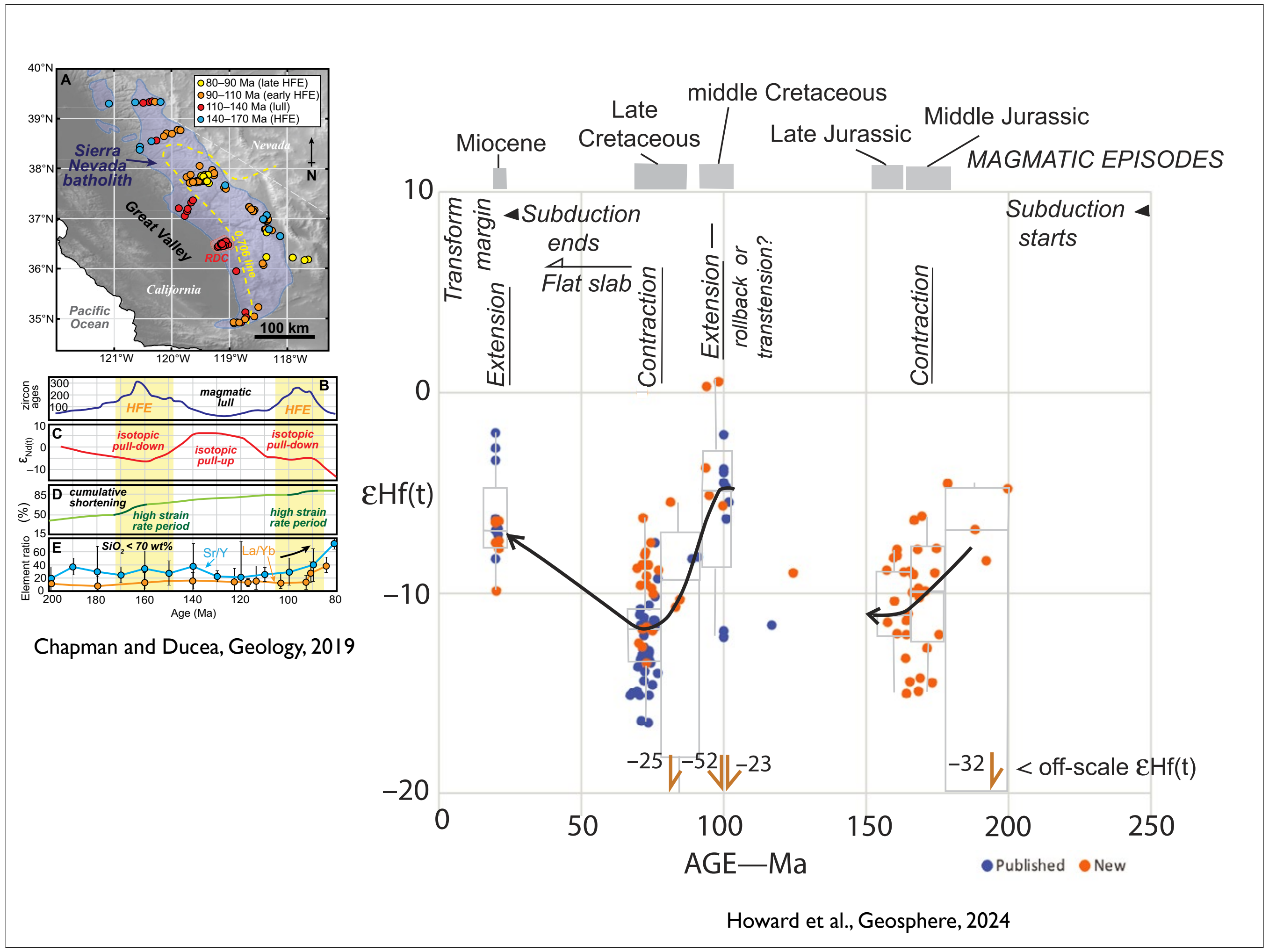

Cycles in the Mojave Desert south of the Sierra. Note “pulldowns” c 75, 155 Ma inferred here to be with contraction like Sierra.

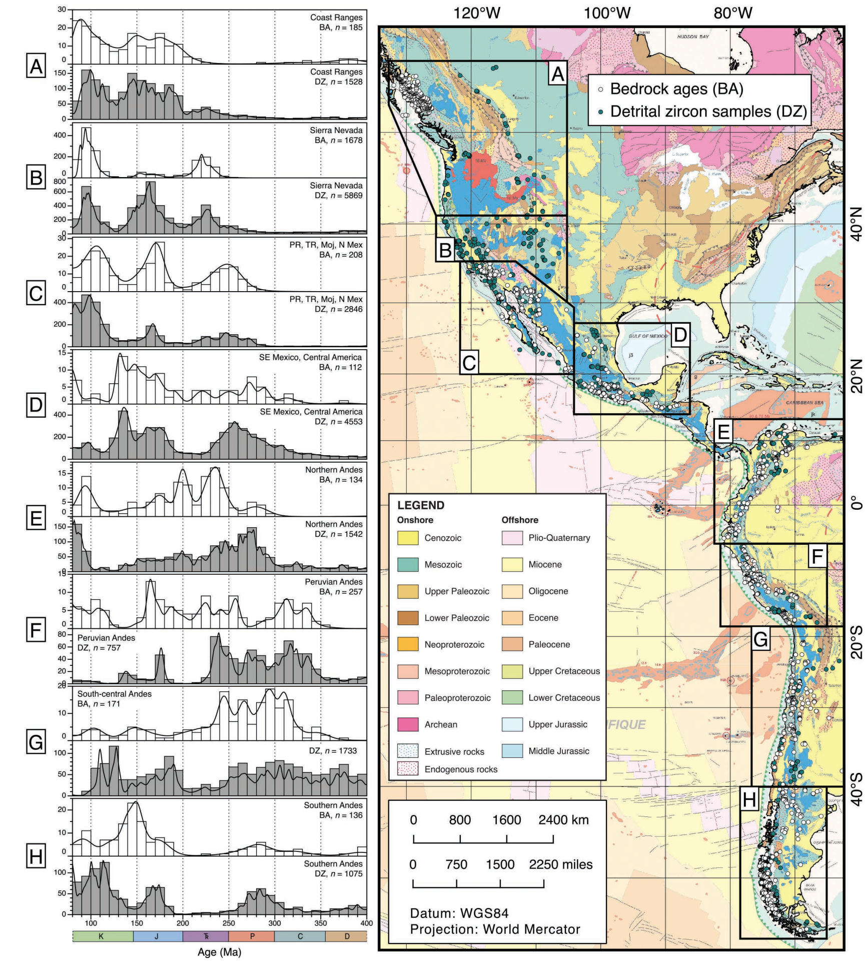

Kirsch et al., *Amer. Minerol.*, 2016

When you look at entire Cordillera, seems controls are variable…so maybe some of the stories told in WUS are confusing coincidence with causality. Do these episodes correlate with plate kinematics?

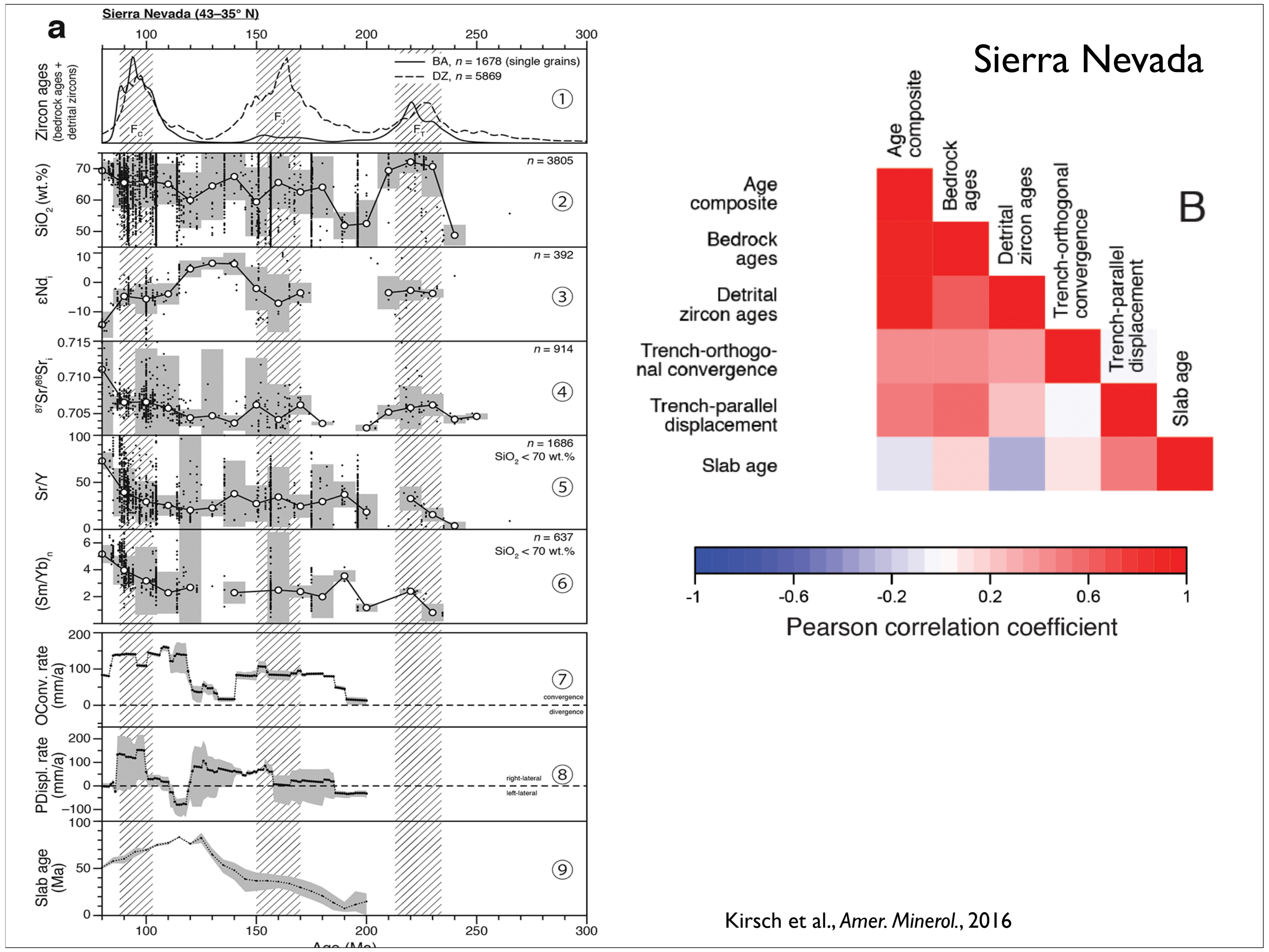

More recent attempt to look at cycles through entire Cordillera. This just Sierra part. Diagonally hatched bands mark magmatic flare-up events, visually delineated on the basis of peaks in the age spectra. For geochemical data, individual data points are plotted (dots), along with median values ±1s (circles and gray bars) for a moving 10 m.y. average. For kinematic data, black dots are average values and gray envelopes represent minimum–maximum ranges from a set of three values extracted per arc domain. Note differing age range in c. Abbreviations: BA = bedrock ages, DZ = detrital zircons, OConv. = orthogonal convergence, PDispl. = parallel displacement.

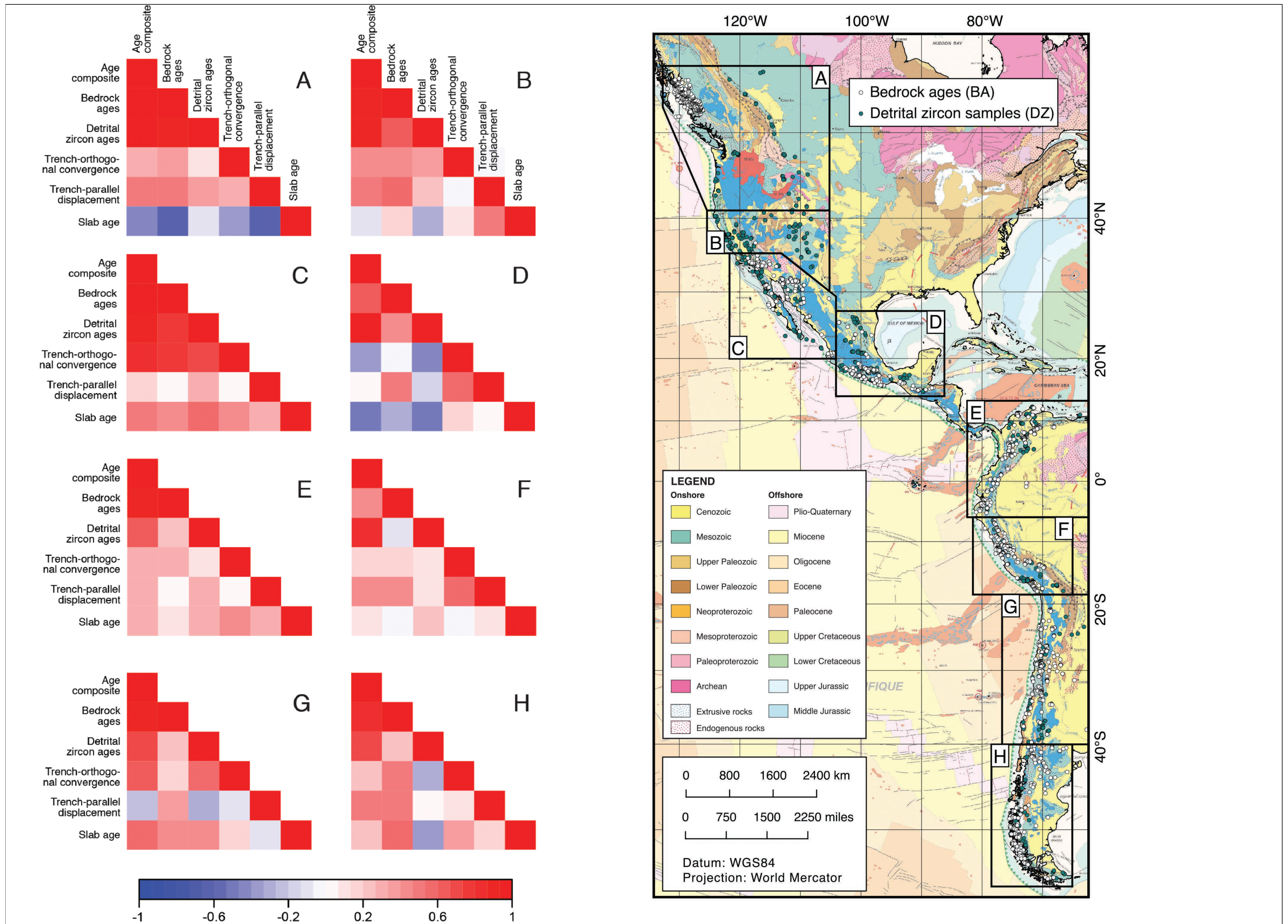

Kirsch et al., *Amer. Minerol.*, 2016

When you look at entire Cordillera, seems controls are variable…so maybe some of the stories told in WUS are confusing coincidence with causality

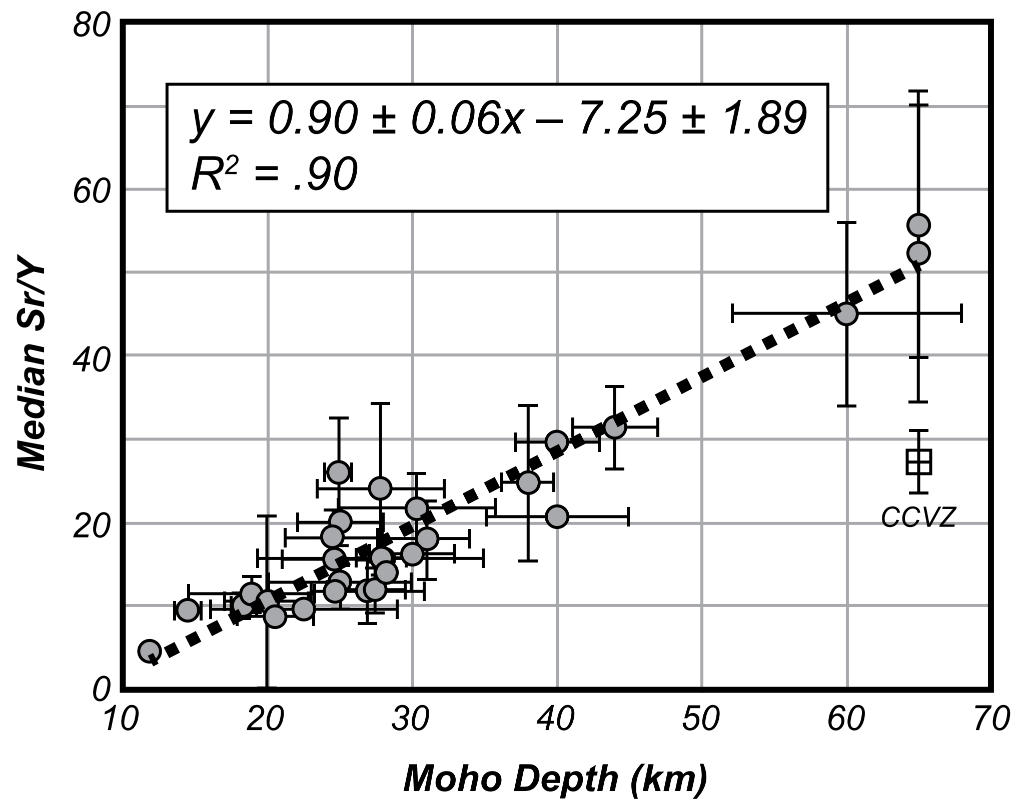

Chapman et al., Geology, 2015

Are these episodic arc flareups expressed in arc thickness? How would we know? Also, why would this work? Sr like solid at low pressures, melt at high (when plag goes away); Y the opposite (likes garnet and amphibole at high pressure).

Figure 2. Global correlation between geophysically determined Moho depth and median Sr/Y from Pliocene and younger magmatic arcs, compiled from GEOROC database (georoc.mpch-mainz.gwdg.de/georoc/). Median Sr/Y was calculated using same filters and processing steps as applied to Great Basin data. Data regression includes all data except central segment of Central Volcanic Zone (CCVZ) in the Andes; see text for discussion. Com- piled data are included in Tables DR4 and DR5 (see footnote 1).

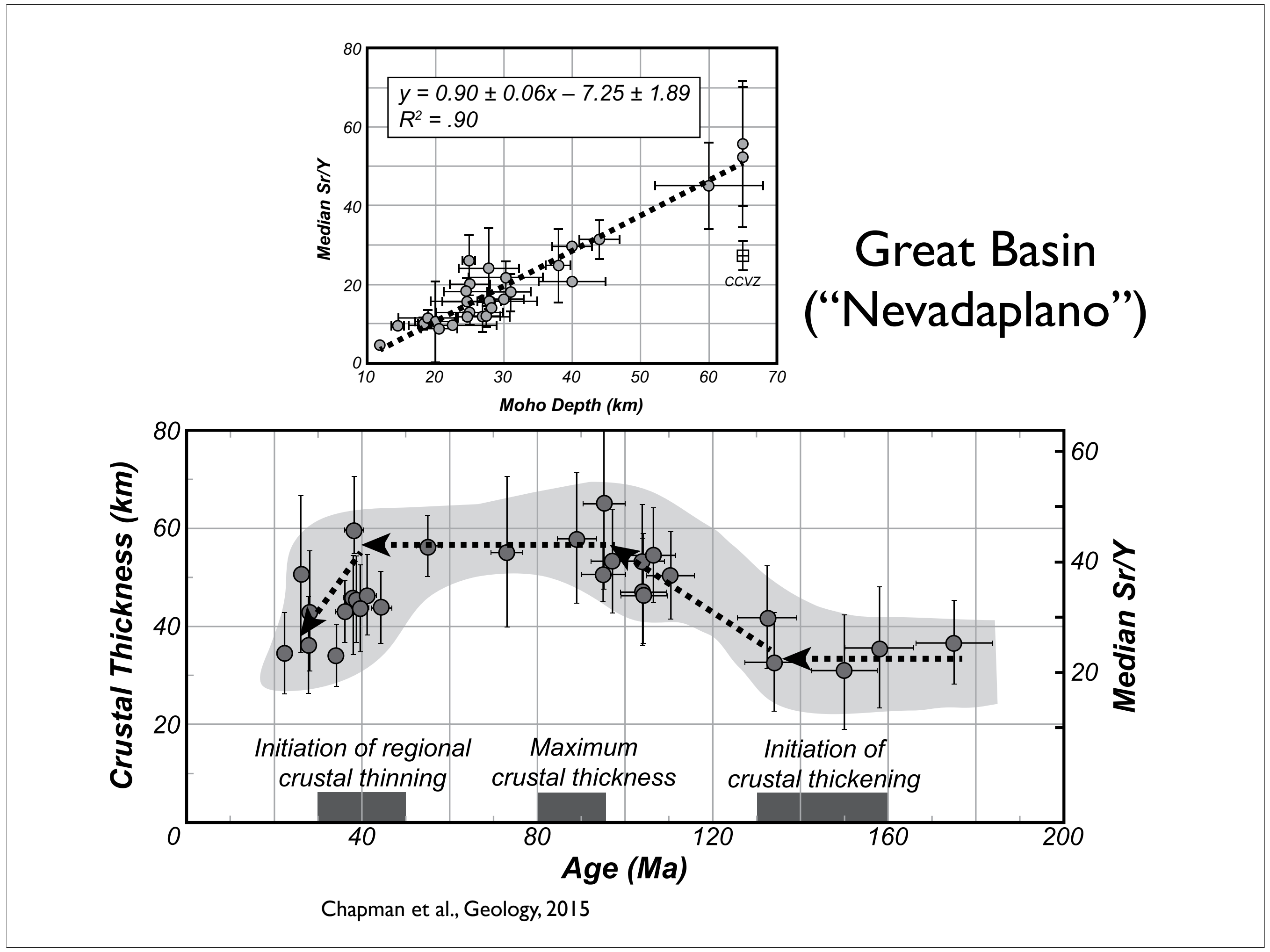

Apply to Great Basin (hinterland)

Figure 3. Plot of changes in median Sr/Y in magmatic rocks and calculated crustal thickness through time for Great Basin region. Shaded region and dashed arrows show interpreted trends in data. Timing for events listed at bottom of plot is constrained by in- dependent geologic studies; see text for discussion. Compiled and plotted data are included in Tables DR1–DR3 (see footnote 1).

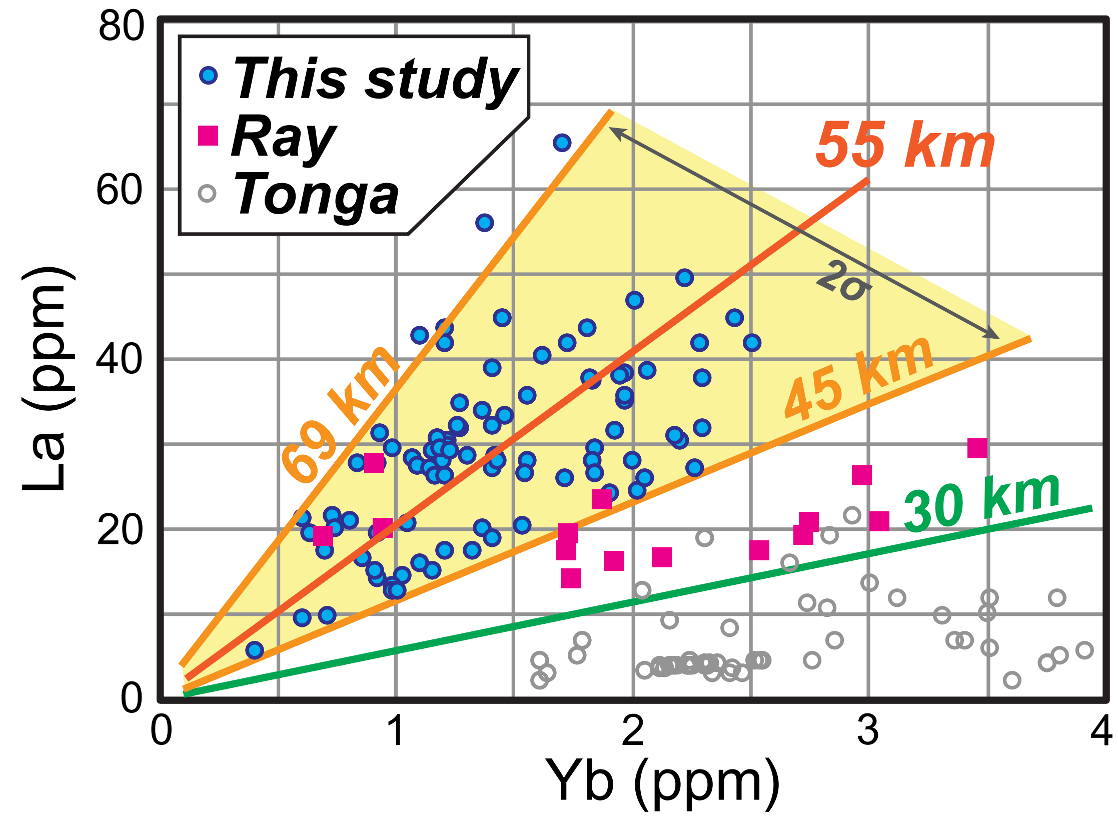

Chapman et al., Geology, 2020

Another proxy: La/Yb for intermediate rocks. This is similar in logic (but empirical) “As crustal thickness increases, whole-rock heavy rare earth element (HREE) concentrations decrease and light rare earth element (LREE) concentrations increase, due to the high-pressure stabilization of HREE- enriched phases such as amphibole and garnet at the expense of LREE-enriched phases such as plagioclase (Hu et al., 2017; Müntener and Ulmer, 2018). Despite the low concentration of LREE in plagioclase, the mineral is impor- tant because of its abundance in continental- arc rocks and because it is unstable at higher pressure, in contrast to other LREE-bearing accessory phases such as monazite.”

Intermediate (see text for discussion of geochemical filters) whole-rock La and Yb data used in this study (blue filled circles), data from the Ray Cu-porphyry system (Arizona, USA) (pink squares), and data from the Quaternary Tonga arc (gray open circles; compiled from the GEOROC database, http:// georoc.mpch-mainz.gwdg.de). Solid lines are crustal thickness calculated from La/Yb using the empirical relation of Profeta et al. (2015). The modern Tonga arc has a geophysically determined crustal thickness of ~20 km (Contreras-Reyes et al., 2011) and is only shown for comparison.

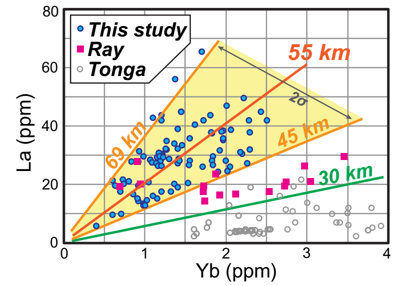

Sonoran Desert
("Arizona-plano")

Chapman et al., Geology, 2020

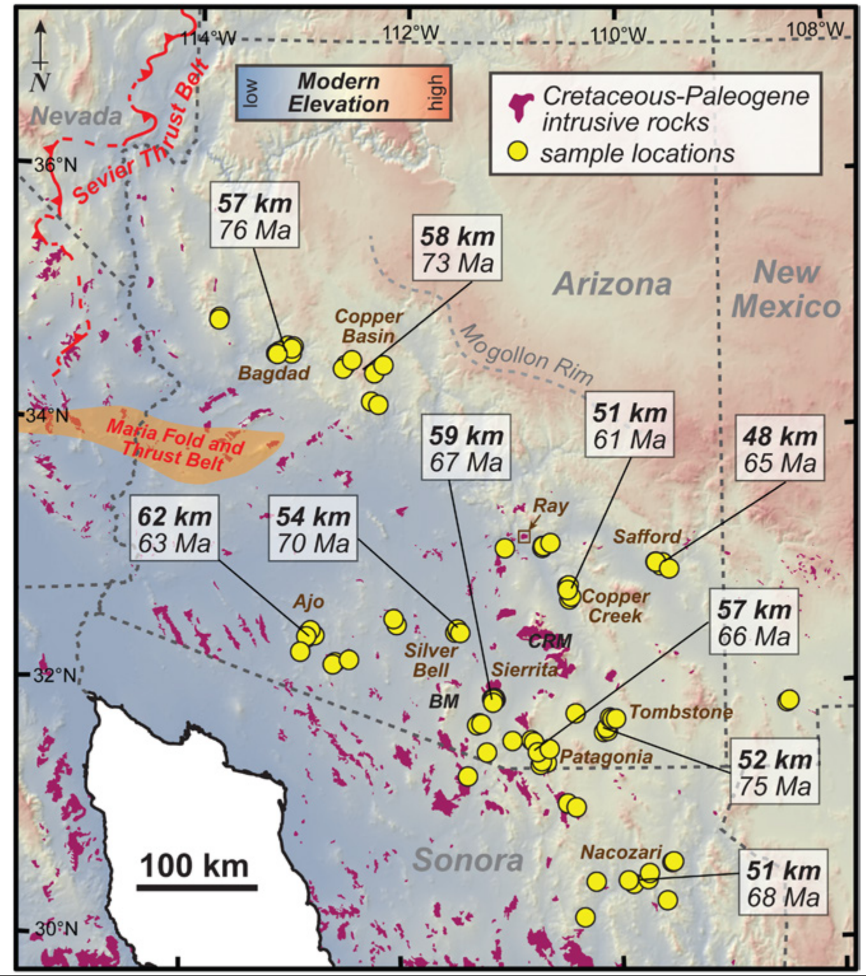

Another proxy: La/Yb for intermediate rocks.

Intermediate (see text for discussion of geochemical filters) whole-rock La and Yb data used in this study (blue filled circles), data from the Ray Cu-porphyry system (Arizona, USA) (pink squares), and data from the Quaternary Tonga arc (gray open circles; compiled from the GEOROC database, http:// georoc.mpch-mainz.gwdg.de). Solid lines are crustal thickness calculated from La/Yb using the empirical relation of Profeta et al. (2015). The modern Tonga arc has a geophysically determined crustal thickness of ~20 km (Contreras-Reyes et al., 2011) and is only shown for comparison.

Comparing Sr/Y and La/Yb

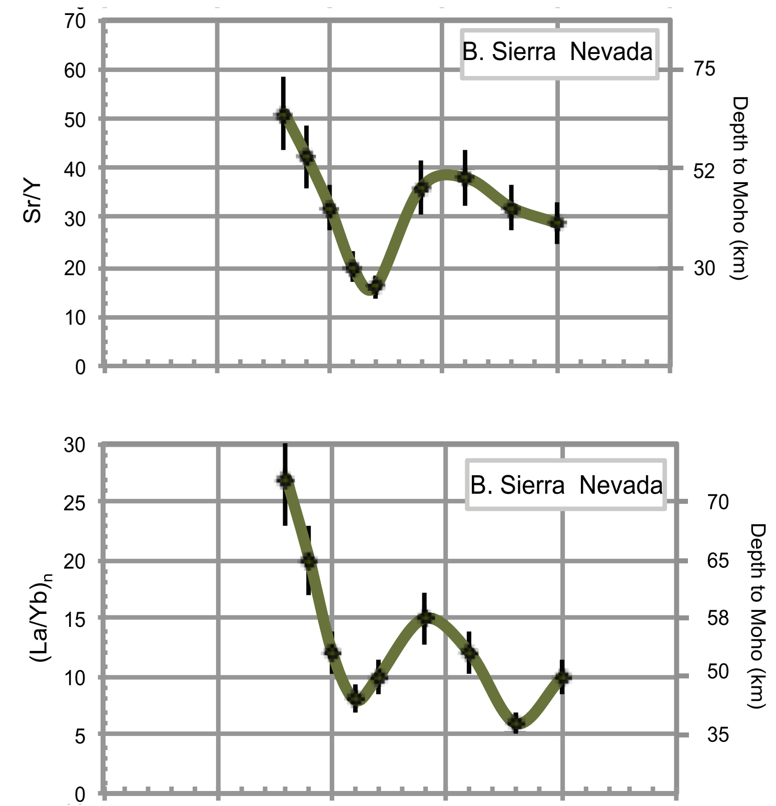

Profeta et al., *Scientific Reports*, 2015

Comparing the two here…

How else might we estimate crustal thickness?

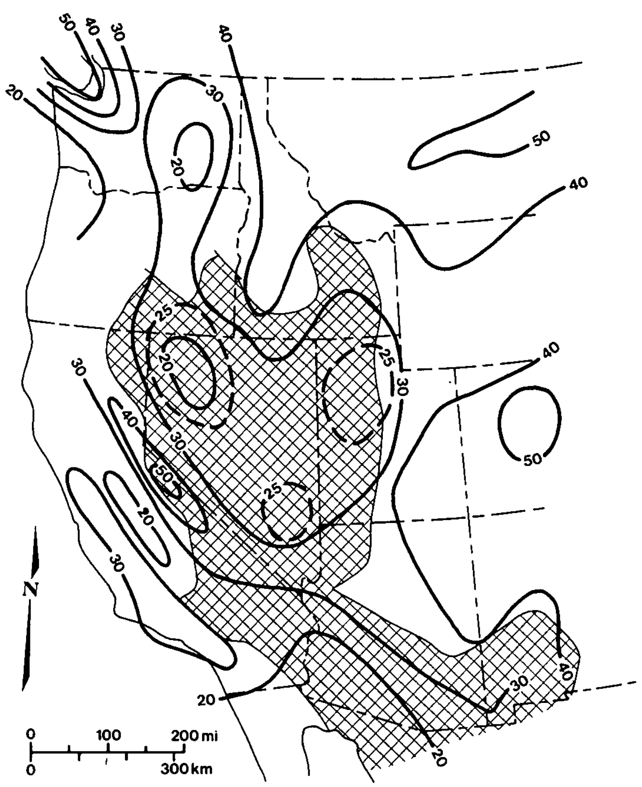

Coney and Harms, Geology, 1984

One of the more influential paleothickness maps…

How else might we estimate crustal thickness?

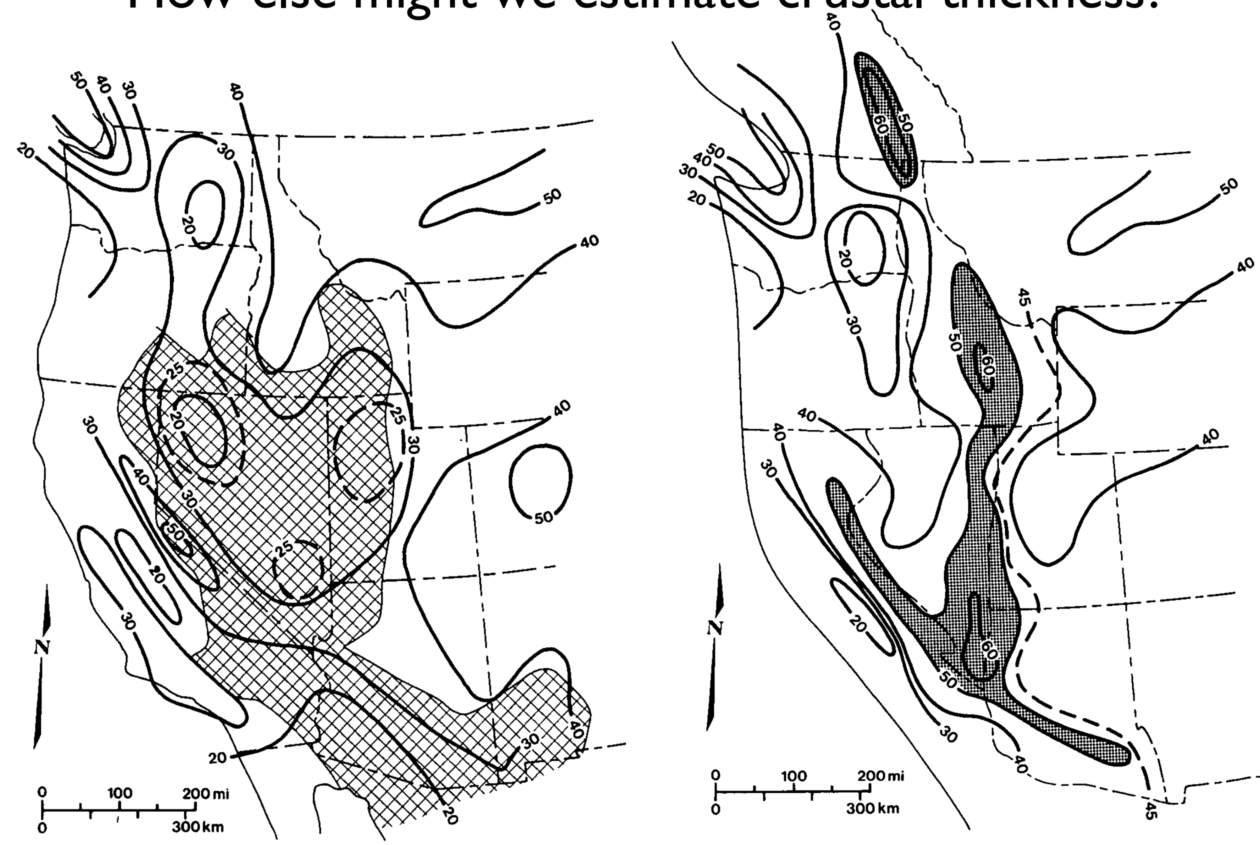

Coney and Harms, Geology, 1984

Simply push everything back. [These are old thicknesses…]

How else might we estimate crustal thickness?

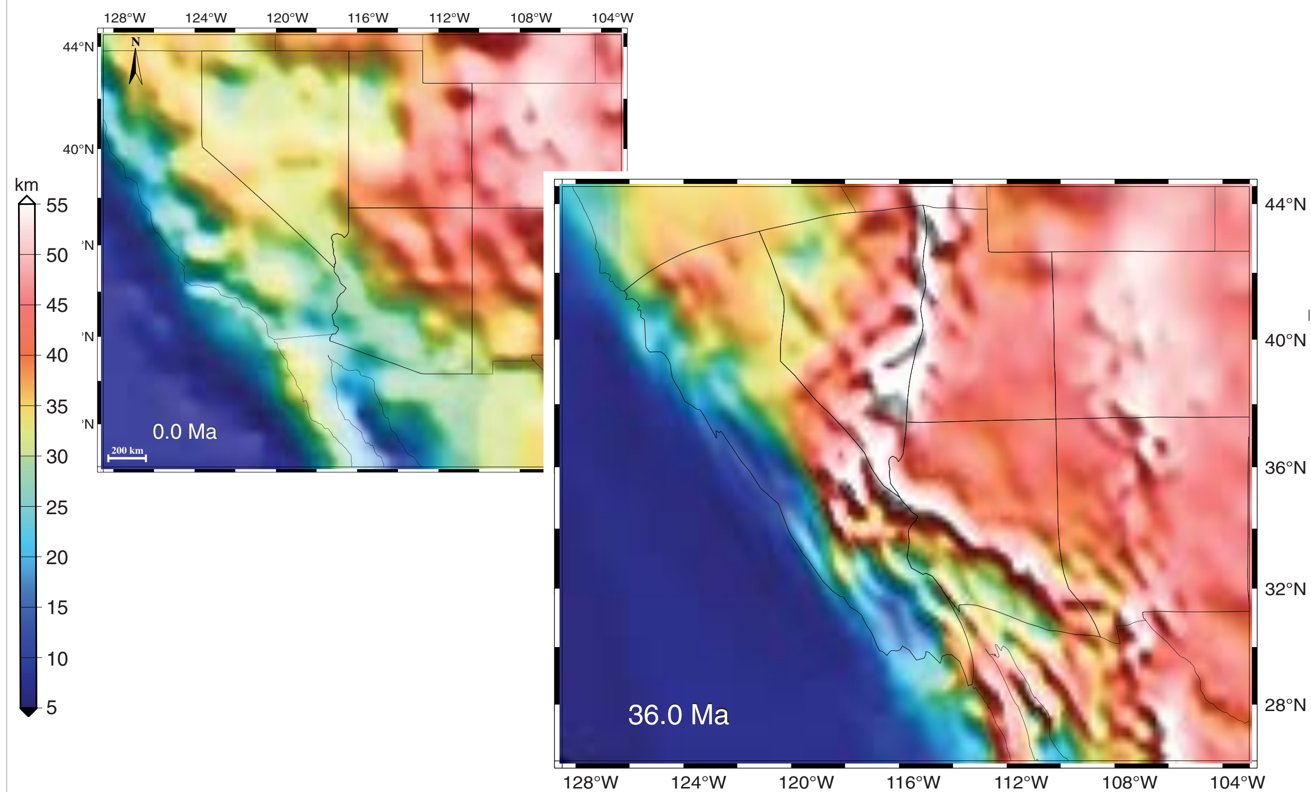

Bahadori et al., Geosphere, 2018

Simply push everything back; a more sophisticated version (and this only gets you to 36 Ma)

How else might we estimate crustal thickness?

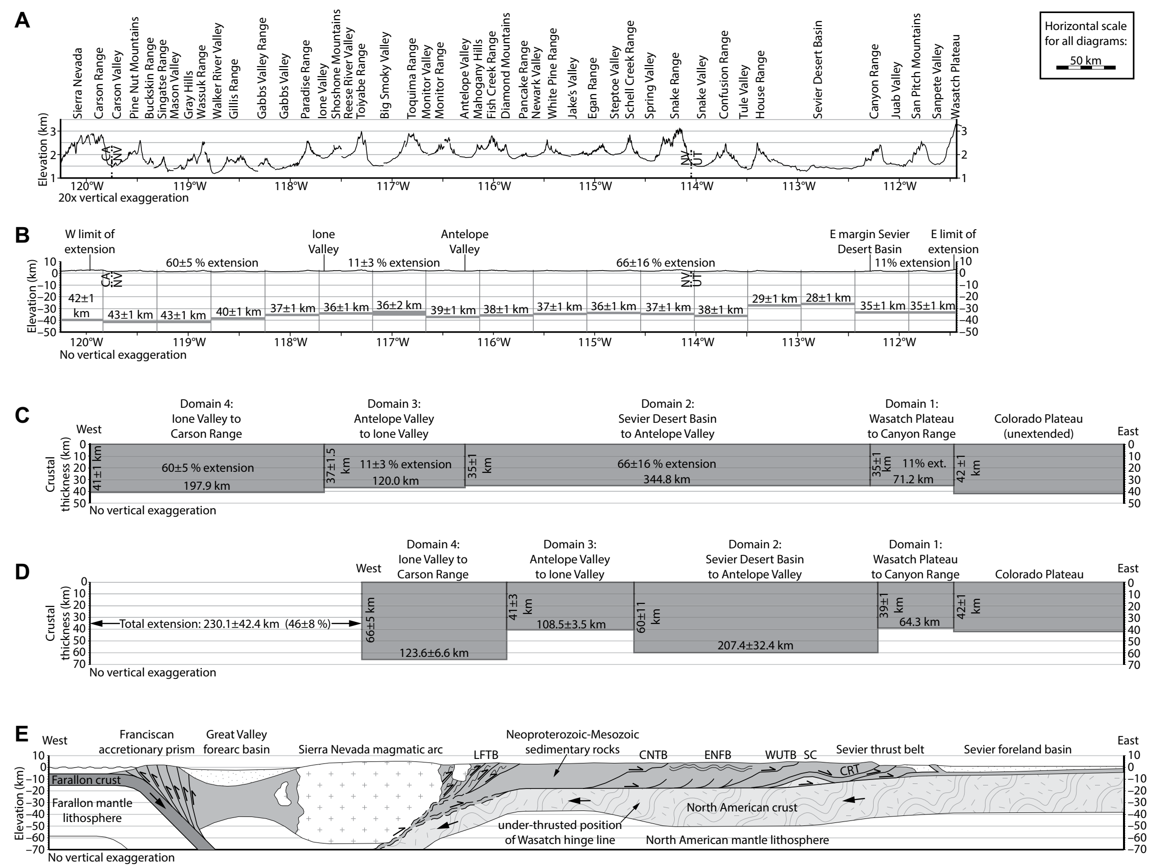

Long, GSA Bull, 2019

Simply push everything back; based on a geological section across the Great Basin.

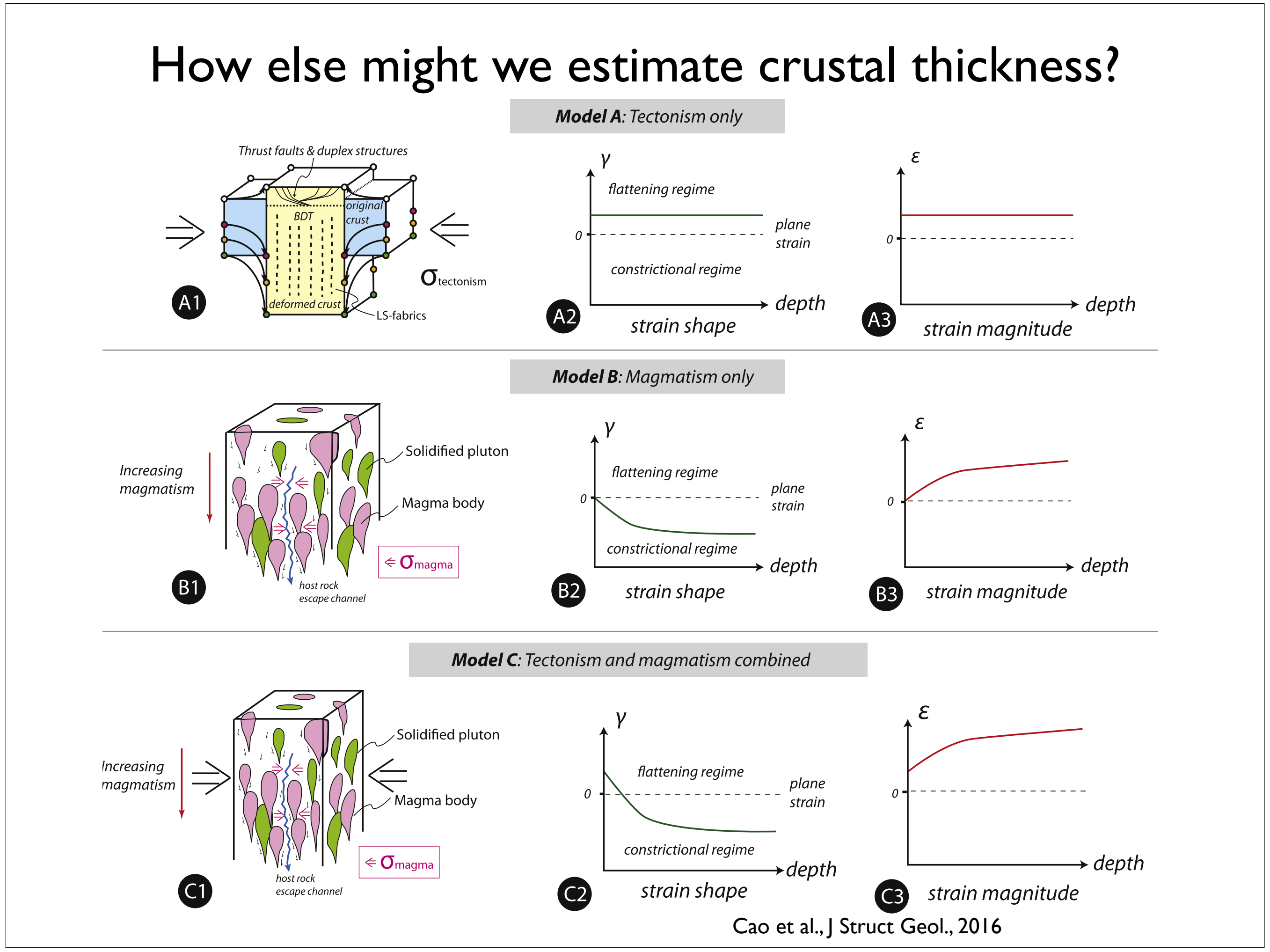

Can try using strain markers and magma volumes…

Three proposed models for ductile straining mechanisms. Model A is homogenous tectonic thickening only. Model B only has the magmatism. Model C combines tectonism and magmatism. A1, B1, and C1 show the cartoon illustrating the corresponding models. A2, B2, and C2 show predicted trends of Lode's ratio (g), or strain shape, changing with depth. A3, B3, and C3 show predicted trends of strain magnitude (ε) changing with depth. See text for full discussion. BDT ¼ Brittle-ductile transition.

How else might we estimate crustal thickness?

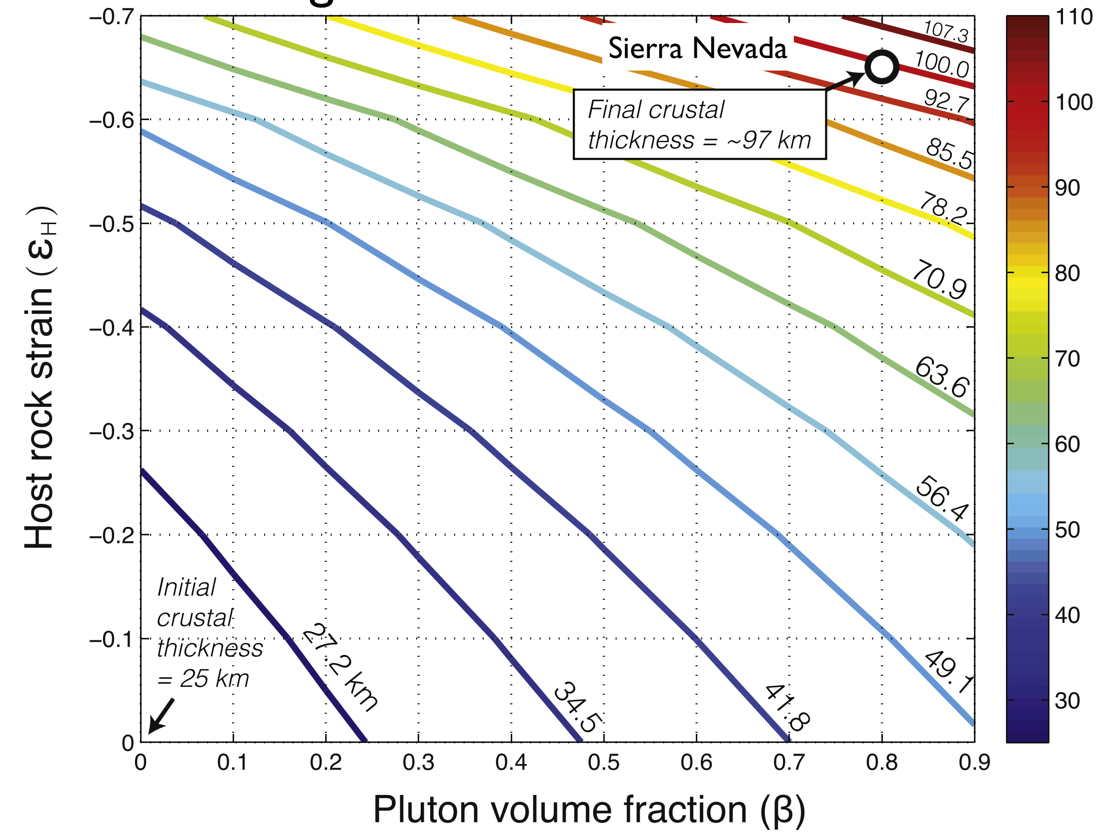

Note, exhumation not included

Cao et al., J Struct Geol., 2016

Can try using strain markers and magma volumes…

Crustal thickness determined by host rock strain (εH) and pluton volume fraction (b). The initial thickness of the crust is assumed to be 25 km and the calcu- lation takes 20% shortening in plutons and 20% volume loss/length change along Y- direction of host rocks into account. If εH 1⁄4 −0.65 and b 1⁄4 0.8, the resulting thickness of crust is ~97 km. The crustal thickness show in this plot does not include exhumation. Exhumation will reduce the thickness to 77e87 km for Late Cretaceous Sierra Nevada

Maybe this matters for more than just arc…

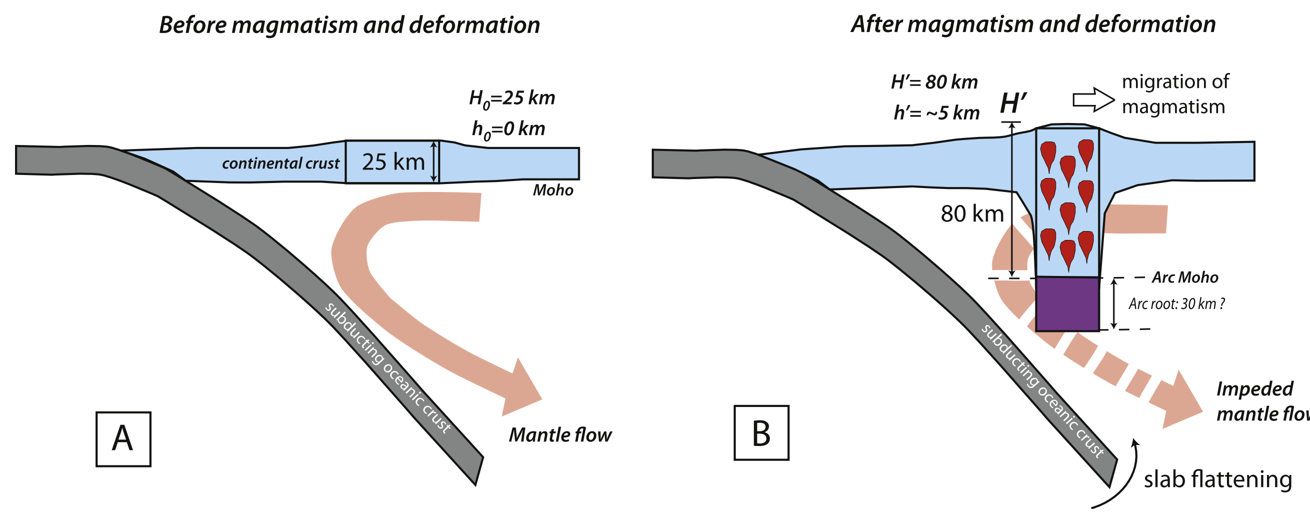

Cao et al., J Struct Geol., 2016

Keep in mind when we talk about dynamic topo and arc shutdown, etc.

Cartoon shows how magmatism and deformation thicken the crust. (A) is the geometry of an arc system before magmatism and deformation. The initial thickness of crust (H0) is 25 km and elevation (h0) is at sea level (0 km). The mantle flow is not impeded. (B) is the geometry of the arc system after magmatism and deformation and it may apply to the Sierra Nevada arc at ~85 Ma. Crust is thickened (H') to ~80 km and elevation (h') is ~5 km. The total thickness of crust and arc root extending into mantle wedge is ~80 km. Mantle flow is impeded. The thickened crust could also cool down the mantle wedge. The impeded mantle flows, cooling effect, and the slab flattening are likely to contribute to the migration of magmatism.

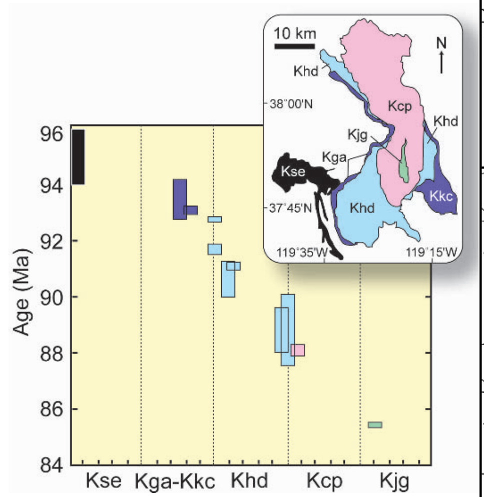

Glazner et al., *GSA Today*, 2004

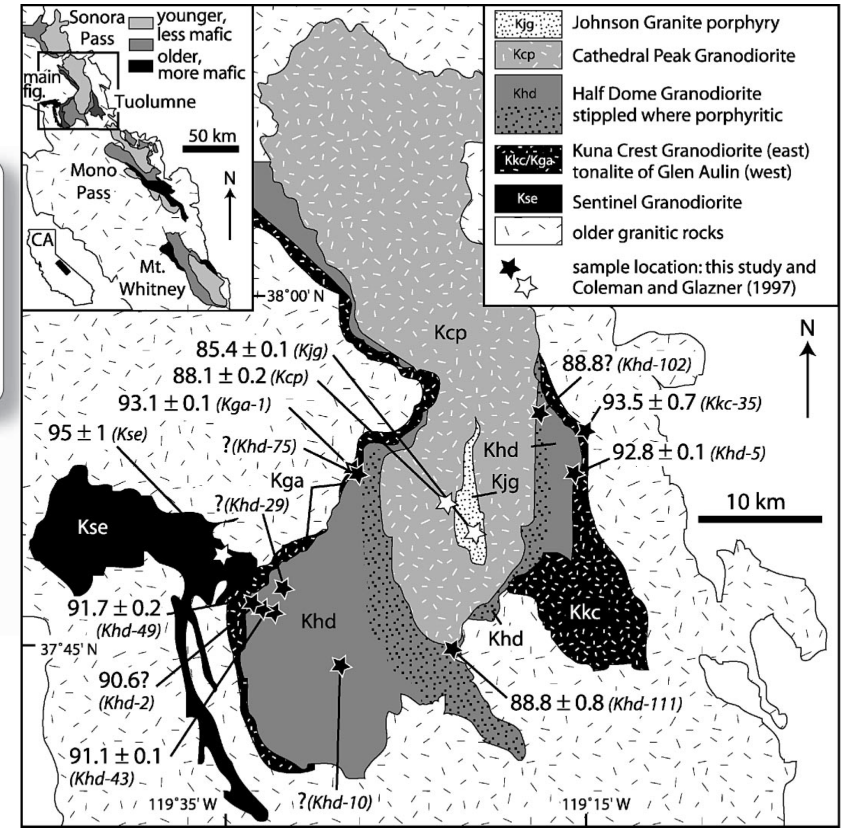

Coleman et al., *Geology*, 2004

On to something different if time. Have been finding with increasingly high resolution dating that plutons are in some cases very long lived. This groups suggestion is that plutons are built more by successive intrusions and not a big cauldron

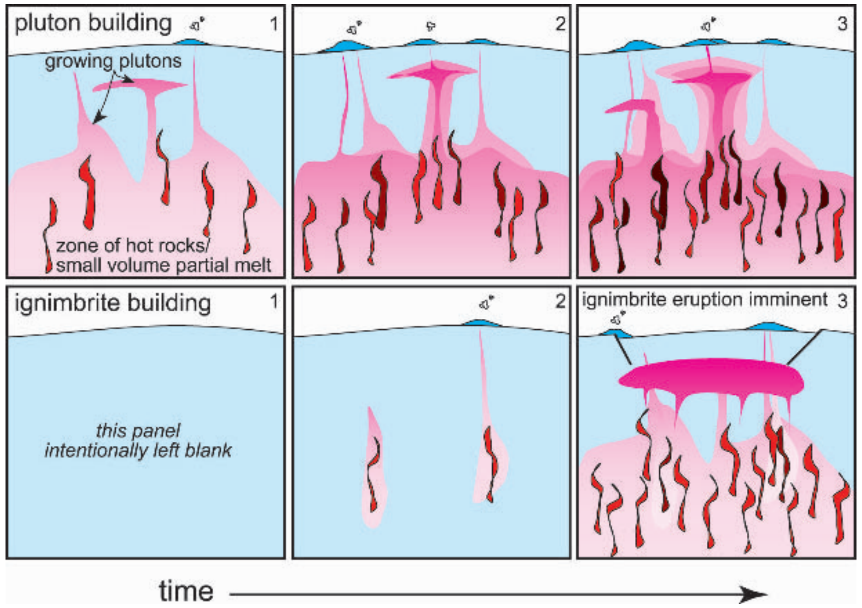

Glazner et al., *GSA Today*, 2004

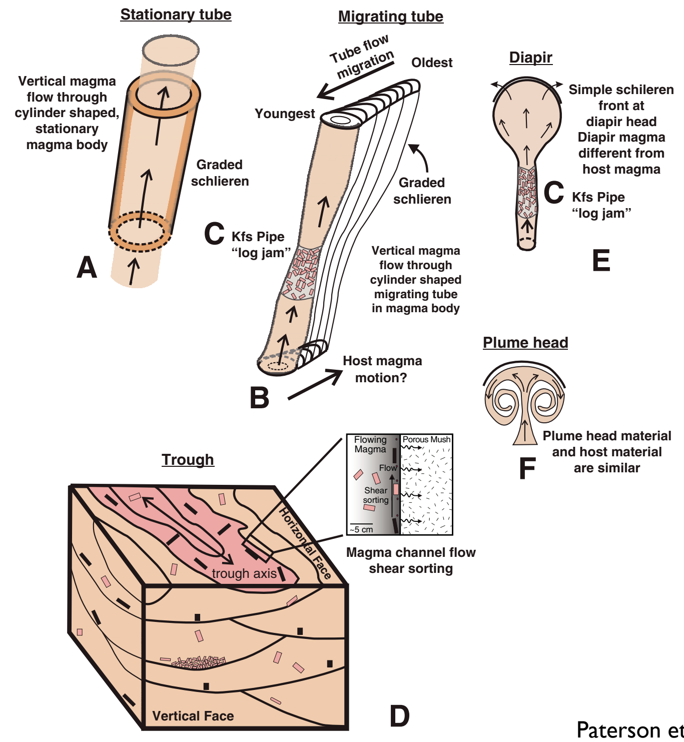

Paterson et al., *Geosphere*, 2009

Figure 18. Features discussed in this paper, possible relationships between different types of structures, and the relationships between mineral fabrics and accumulations. (A, B) Tubes. (C) Pipes; Kfs—K-feldspar. (D) Troughs. (E) Diapirs. (F) Plume heads. Some drawings are based on diagrams in Weinberg et al. (2001), but with a number of additions. Trough illustrations show typical relationships between trough cutoffs, mineral fabrics, magma flow directions, and crystal accumulations seen in the field. Arrows show implied magma flow directions in each structure.

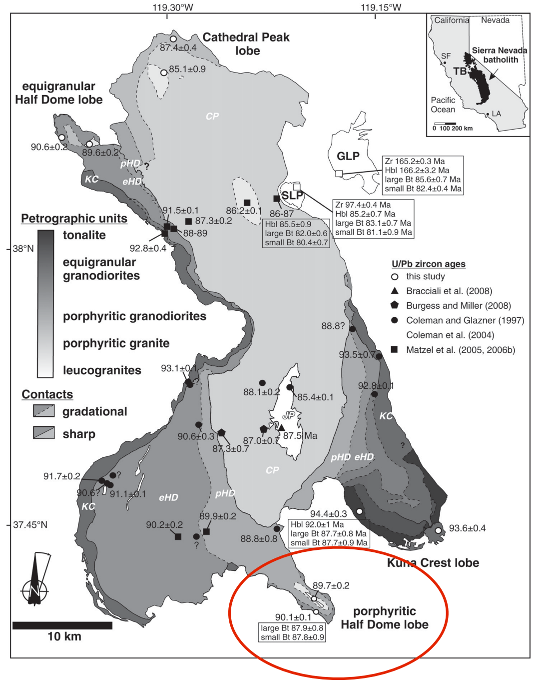

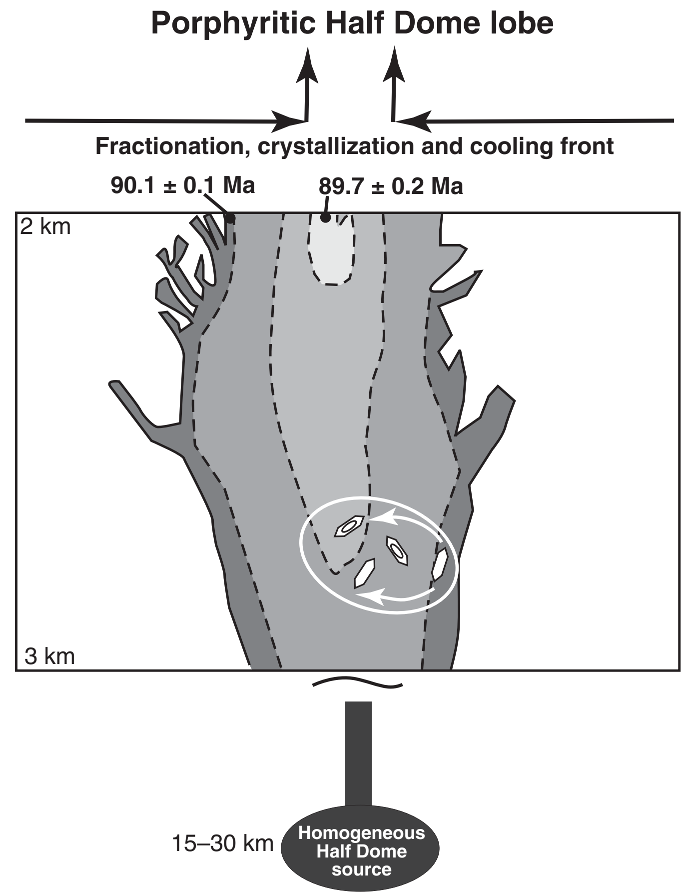

Memati et al, GSA Bull, 2010